Innovative Temperature Sensing PCB Design and Data Collection

Juan Sigman
3rd year MEng Electronic Engineering
King's College London
juan.sigman@kcl.ac.uk

Gerard Montblanch
3rd year MEng Electronic Engineering with Management
King's College London
gerard.montblanch@kcl.ac.uk

Emir Mukovic
3rd year MEng Electronic and Information Engineering
King's College London
emir.mukovic@kcl.ac.uk

Nathaniel Williams
3rd year MEng Electronic Engineering
King's College London
nathaniel.1.williams@kcl.ac.uk

Anas Baig
3rd year MEng Electronic and Information Engineering
King's College London
anas.baig@kcl.ac.uk

Originality Avowal

We can confirm that the work in this paper and project is entirely our own. Anything obtained from other sources is referenced and can be seen in the bibliography. We grant the right to King's College London to make paper and electronic copies of the submitted work for purposes of marking, plagiarism detection and archival, and to upload a copy of the work to Turnitin or another trusted plagiarism detection service.

Acknowledgment

We would like to thank Dr.Guo Miao for all of her help in the organization and execution of this group project. We certainly could not have achieved what we did without her. Furthermore, we would like to thank James Kong, Tom Hobson, Bashir Al Droubi, Jared Bellingham and everyone else at Alp Technologies for allowing us to work side by side with them and helping us design and test our final product.

A note on figures

Every unreferenced figure in this paper was created by the authors, either in MATLAB or in PowerPoint.

Contents

List of Figures

List of Tables

***Abstract*—Alp Technologies is an engineering startup working on a modular battery system called the BRIC. One issue with this battery pack is that, in the case of a fault, the company is unable to pinpoint what cell is causing these issues. In this project, we aim to introduce temperature sensors into the BRIC to aid in the detection of faulty cells in the system. After designing the new BRIC, we went on to test it and provide a prototype that the company could implement if desired.**

***Index Terms*—Energy storage, renewable energy, temperature sensing, Alp Technologies**

I. Executive Summary

Alp Technologies is an engineering startup working on a modular battery system called the BRIC. One key characteristic of the BRIC is its ability to incorporate both new and old cells, as well as cells from different brands, greatly reducing cell waste. One issue with the battery pack is that, in the case there is a faulty cell, it is unable to pinpoint where exactly that cell is. Taking into account that faulty cells tend to heat up, it is a fair assumption to think that the faulty cell in the BRIC would be the warmest. Because of this, the ultimate goal of our project is to introduce temperature sensors in the BRIC. Then, in the case that there is a problem with the BRIC, we can simply look at the temperature of each cell and most likely, the warmest cell will be one causing the issues.

In order to complete this project, we designed a four–step plan. The first step was simply to go into the Alp Technologies offices and build BRICs. This gave us a deep understanding of how the BRIC works and how all of its smaller pieces work together.

The second step in our plan was to perform experiments on the BRIC as well as individual cells to attempt to understand how they behave under different loads. This gave us an insight on the temperature curve of the BRIC, giving us the tools to go on to design our final product.

The next step was the actual design of the PCB in the Altium software. This involved landing on a final design and circuitry for our product, choosing the components, designing the schematic and finally placing all of the footprints on the PCB. As this was happening, we also worked on a code to be able to read the data from the temperature sensors in the BRIC.

Finally, the fourth and final step in our project plan was to test the design. This involved going to the offices to assemble the BRIC to then perform several experiments on it to test its behaviour and functionality.

II. Introduction And Background

A. Universal Need for Electricity

Every day, we are surrounded by one of the most essential discoveries of all time; electricity. While it is possible to survive in a world without this good, our modern day society practically demands we have a stable access to it. Our daily lives are constantly affected by electricity. Homes are powered by it, which allows us to cook, clean or turn lights on, among other things. Moreover, it is also omnipresent, appearing everywhere one might go.

However, while developed countries have the pleasure of enjoying electricity due to their technical capabilities, there are over 100 million people in sub-Saharan Africa without access to it [1]. Their lives are constantly affected due to the energy crisis many African countries suffer, having less availability to several necessary services such as hospital resources or schools.

An important milestone in today's day and age are the UN's seventeen Sustainable Goals to be completed by the year 2030. Specifically, the seventh goal aims to [2]: Ensure universal access to affordable, reliable and modern energy services; substantially increase the share of renewable energy in the global energy mix; and double the global rate of improvement in energy mix.

As can be seen, the UN already has its eyes on improving the energy situation in underdeveloped countries. Companies like Alp Technologies are working towards the joint completion of this goal and hopefully it will be achieved by the end-date of 2030.

B. Renewable Energy

Due to environmental concerns, worldwide renewable energy usage has been steadily increasing, in fact, it is becoming the fastest growing energy source. The share of renewable energy in global electricity generation was 27% in 2019, jumping to 29% in 2020. Additionally, there was an expected expansion of 8% in 2021, reaching a total generation

of 8300TWh, making it the fastest year-on-year growth since the 1970s

The climate conditions in Africa allow for an enormous opportunity for renewable energy generation. The International Renewable Energy Agency estimates that renewable energy capacity could reach the 310GW in Africa by 2030, placing the continent at the top of renewable energy generation globally. Fig. 1 shows the share of renewable and fossil fuel generation capacity in Africa by region [3].

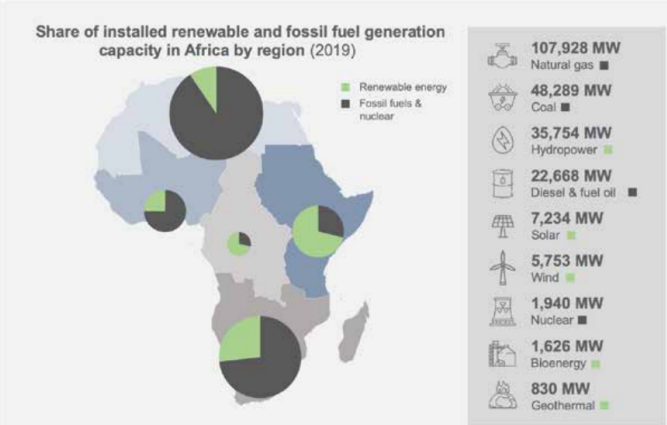

Fig. 1: Share of renewable and fossil fuel generation capacity in Africa by region [4]

The potential for renewable energy generation in Africa is arguably the largest in the world due to its natural resources. Sunlight is generously available across the entire continent, while other resources such as wind or running water (hydro power) are more abundant in specific areas.

1) Solar photo voltaic: More than 80% of African land receives north of 2MWh per year per squared meter of sunlight. Irradiation levels are double compared to Germany, making it a resource that can bring power to rural areas without the need of expensive materials.

2) Hydro power: The hydro power potential in Africa is currently more than 90% unexploited, with it having the potential of an estimated $1478\frac{\text{TWh}}{\text{year}}$. The largest share of hydro power is Central Africa with a 40%, followed by East Africa with 28%.

3) Wind power: Wind power can mainly be exploited in the coastal areas of Northern Africa, Southern Africa and Eastern Africa due to their exceptional wind resources.

4) Geothermal power: Geothermal power has a potential of 15GW of installed capacity and $105\frac{\text{TWh}}{\text{year}}$. The main geographical area for this resource is generated in the Rift Valley in Eastern Africa.

5) Biomass power: Nowadays, biomass power generation in Africa is almost non-existent. However, there is a considerable potential for this type of power in central Africa, having the possibility of reaching the values of $2374\frac{\text{TWh}}{\text{year}}$. This represents a huge opportunity for renewable energy generation aimed for heavy manufacturing, as it can be used to produce process heat.

C. Electricity Access in Africa by regions

The share of Africans with access to electricity at home has increased from 36% in the year 2000 to 54% in 2018. Even though this increment has been substantial, there are still around 548 million people in the whole continent living with no electricity. Moreover, different African regions have widely different access to electricity. Table I below shows the percentage of electrified people in the different regions in Africa in 2018 [5]:

TABLE I: Electricity access in Africa regions

Region	**Population** (millions)	**%electrified**	**People without energy** (millions)
Northern Africa	199	98%	4.7
East Africa	359	47%	188
Central Africa	138	30%	97
West Africa	376	53%	178
Southern Africa	203	51%	99

D. Energy Storage

While it is important to be able to produce energy, another concept that is as important is to store it for later use. There are several methods of doing this, the main one in Electronic Engineering being the use of rechargeable cells (usually Lithium–Ion). These cells can be put together in a circuit to form a battery.

One current issue with batteries is that, if there is a problem with one of the cells, usually the whole battery has to be discarded. This results in both cell waste, which is a significant issue in our current society, as well as energy waste. Furthermore, it is strongly recommended to use the same type (brand) of cells within them.

E. Alp Technologies

A company that has been working on the previously mentioned problems is Alp Technologies. They are an engineering start-up focused on developing renewable energy technologies for low-income countries. Their products not only are needed in underdeveloped countries due to energy crisis, but also essential for the whole world. Alp Technologies compete in one of the most innovative markets as their products can have a great impact on building the new generation of renewable energy technologies.

F. The Mega-BRIC

The Mega-BRIC developed by Alp Technologies is a modular battery system comprised of battery packs called BRICs. Each BRIC consists of 40 cells in a 4p10s configuration. Fig. 2 below shows the circuit diagram for the BRIC.

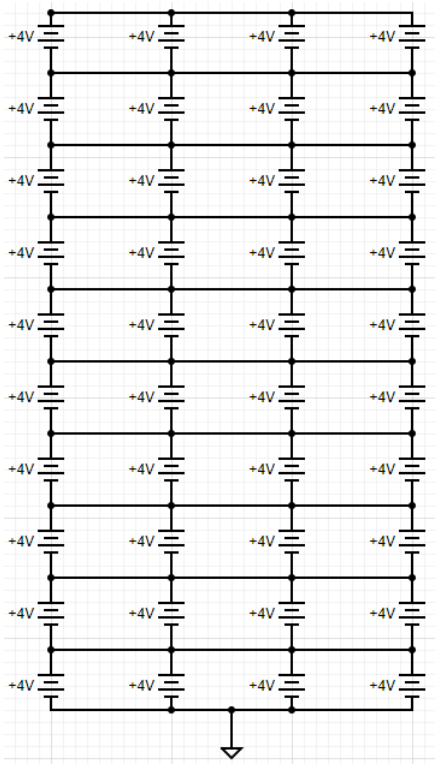

Fig. 2: Circuit Diagram for the BRIC

While ideally every cell is charged at $4V$, this is not always the case. Each cell is actually charged to any value between $3.8V$ and $4.1V$. The BRIC also has an analyser board responsible for monitoring its performance in terms of their energy storage, discharge and other factors such as the current and voltage in the system. To avoid problems related to the imbalance of the charge on the cell, the analyzer board also measures and balances the row voltages so they are equal.

Four BRICs can be connected together to create a 16p10s battery that can work on just one analyser board. Once again, the analyser board monitors the BRIC's performance and balances the row voltages. This modularity is key in enabling the scalability in the future and a 30% cost advantage per unit storage, as well as ease in both maintenance and assembly [1].

A defining feature of the M–BRIC (and BRIC) is its ability to incorporate both new and used cells in the system as well as cells from different brand, which will reduce battery landfill and provide flexibility for the user.

G. The issue

One issue with the BRIC arises if a faulty cell is present in the system. Through the row voltages, the BRIC can only pinpoint what row the cell is in, not which specific cell it is. This can lead to either cell waste, as the entire row needs to be discarded due to a single faulty cell, or time waste, since each individual cell would have to be tested in the row. This issue becomes more consequential with the 4–BRICs–per–analyser–board system, as now the faulty cell can only be specified to one out of 16.

Battery cell waste, a subcategory of e–waste[1], has become a considerable environmental problem. According to the United Nations, between 2014 and 2019, the global e-waste volumes grew by 21% and just in 2019 the world discarded 53.6 tons of e–waste, with only 17.4% of ot being recycled.

Due to the amount of electric vehicles, computers and other objects that require batteries to function, the United Nations estimates that global e–waste volumes could increase to 74.7 million tons per year by 2030, a 39% increase from current values [6].

One solution to this problem is to introduce temperature sensors into the BRIC. Faulty cells tend to overheat, therefore if the analyser board flags a

[1]Formal definition of e–waste is any electronic waste that is no longer wanted or is now obsolete, whether it works or not

problem in one of the rows, the temperature of each cell within the faulty row can be observed. It then is most likely the cell at the highest temperature will be the defective one.

III. Literature review

There is a wide variety of academic papers on the topics we are working on available to everyone. Throughout the execution of our project we have analysed the available literature to try to gain a grasp on what has been explored in the field and what has not. More specifically, we read papers relating to three different topics.

A. Opportunities for the M–BRIC

As was mentioned earlier, the energy potential in Africa is arguably the largest in the world. Several academic papers explore this potential and give frameworks to exploit this potential. For example, the paper *Conceptual Framework for Sustainable Energy Development in Africa* [7] provides a theoretical model to purvey sustainable energy to the continent. In the article, the author mentions several key elements that need to be modified or improved in order for the scheme to work. Some examples of these are education, measurement and monitoring or the implementation of renewable energy. This is a very interesting concept, specially when put together with the M–BRIC. This aspect of it has not yet been explored, and it would be interesting to see what role the M–BRIC plays in the proposed framework.

While there is no literature relating specifically to Alp Technologies, there are several papers that go into different battery systems that could be used in Africa to produce sustainable energy for homes. For example, the article *Sustainable Energy Storage for Solar Home Systems in Rural Sub–Sahaan Africa – A Comparative Examination of Lifecycle Aspects of Battery Technologies for Circular Economy, with Emphasis on the South African Context* [8] looks at three battery systems that could be used in Africa to produce sustainable energy for homes. After exploring the three systems, it was concluded that Lithium–Ion batteries require a very high initial capital investment due to material issues and poor prospects for refurbishment. Because of this, it was established that the best choice was the already used system of VRLA batteries despite low efficiencies and shorter lifetimes. Another battery worth exploring in the topic is the M–BRIC. Its modularity results in much lower implementation and maintenance costs, potentially making it a suitable option over VRLA batteries.

After exploring a wide array of literature relating to the energy potential in Africa, we can conclude that there are many papers that provide conceptual frameworks or future alternatives for the energy development in the continent, something very important and useful. One element that was lacking was how the M–BRIC tied to this. With Alp Technologies being a relatively young company, not many studies have been done on their battery. As time goes on and production increases, the impact the M–BRIC could have in Africa will be explored in more depth.

B. Lithium–Ion Batteries

The next natural step in our research was to explore the behaviour of Lithium–Ion batteries. Since that is essentially what the M–BRIC is, a good understanding of the topic was paramount. There is a wide variety of literature available in the topic, with a lot of emphasis made in the health of such batteries. One such paper is *Effect of temperature on the ageing of Li–Ion batteries operating above room temperature* [9], which explores the correlation between temperature and the degradation of every component in a LiB. It was found that when the temperature increases from 25° to 55°, the degradation rate of maximum charge storage after 260 cycles increases from 4.22% to 13.24%. Therefore, we need to aim to keep the BRIC's operating temperature below this threshold to make sure that no damage is being done to its components.

Another concept that is deeply explored in the current literature is the lifetime extension of Lithium–Ion batteries. This is an important element of battery management, as extending their lifetime results in lower costs. A paper that explores such notion is *Lifetime extension of Lithium–Ion batteries with low–frequency pulsed current charging* [10], in which the authors explore the low–frequency positive pulsed current (PPC) charging method in contrast to previous studies which have only investigated frequencies above 1kHz. To determine the degradation mechanism and cell impedance, the

disassembly–based post mortem analysis was used by the authors, concluding that low–frequency PPC charging should be considered as a promising charging method, with a frequency of 0.05Hz showing the best lifetime prospects.

C. Heat Dissipation in Lithium–Ion Batteries

The basis of our entire project is related to the heat dissipation characteristics of Lithium–Ion batteries. Because of this, we have read many papers related to the topic. Many of these papers come in two steps: simulation and experimentation. As an example, in *Temperature Distribution on Lithium–Ion Polymer Battery: From 12V Module to 48V Pack* [11], the authors first simulate a simple 12V battery system discharging at different ambient temperatures, finding that heat dissipation while discharging is dependent on both the discharge rate and the ambient temperature. This was replicated with an equivalent real–life system, obtaining the same results. To show that these results are scalable, the authors then try the same experiment on a 48V battery pack, finding similar results.

A similar paper to the one mentioned above is *Study on the thermal interaction and heat dissipation of cylindrical Lithium–Ion battery cells* [12]. In the paper, the authors first simulate the discharge of a single cell and analysed its heat generation rate, where they once again found that increasing the discharge rate also increases the heat generation rate. Furthermore, an experiment was performed on a 5p4s battery pack. Once again, it was found that higher discharge rates result in higher heat dissipation.

The article *Heat generation and thermal transport in Lithium–Ion batteries: A scale–bridging perspective* [13] explores a similar concept, with an emphasis on the multi–scale aspect of battery systems, from the microscale electrode components to the macroscale battery packs. Different heat generation sources such as Ohmic heating or reactions at the electrode–electrolyte interface are explored. Once again, they find that heat generation in batteries increases with C–rate[2].

[2]C–rate is defined as the charge/discharge rate divided by the nominally rated battery capacity. A discharge rate of 1C means that the battery discharges completely in one hour.

Lastly, there are articles that also explore the applications of machine learning to the thermal behaviour of batteries. One such paper is *Heat dissipation optimization of lithium–ion battery pack based on neural networks* [14], where the authors explore the spacing and organisation of Lithium–Ion battery cells in a battery pack for better cooling. A Bayesian neural network trained on different battery spacing and maximum temperature together with temperature difference was used to find the best spacing.

There are a lot of academic papers available relating to the topic of heat dissipation in Lithium–Ion batteries. One subtopic that has not been explored as deeply is heat generation in faulty cells. Since Alp technologies use recycled cells, some of them might be faulty. Therefore it would be really helpful to understand the heat generation mechanisms of unhealthy cells.

D. Temperature Measurement Methods in Batteries

Having understood the available literature on thermal generation in batteries, the natural progression is to study ways to measure their temperature. There are many papers exploring different methods of doing this, ranging from simple methods such as using sensors to sensorless temperature measurements based on electrochemical impedance spectroscopy.

A common temperature measuring method is using resistance temperature detectors (RTD). The paper *In Situ monitoring of temperature inside Lithium–Ion batteries by flexible micro temperature sensors* [**?**] explores the use of these sensors to accurately measure temperature rather than traditional thermocouples, as the latter are too large to accurately measure at an optimal position.

More complex methods can also be explored, such as in the article *Recent advancements in fiber Bragg gratings based temperature and strain measurement* [15], where the method of Fiber Bragg Gratings (FBG) is explored. This method can be used for both temperature and strain measurements, and it was found that the method struggled with measuring low temperatures[3], but showed no issues at higher temperatures.

[3]Below 0°

Sensorless methods can also be observed in papers such as *Sensorless battery temperature measurements based on electrochemical impedance spectroscopy* [16], where a new method that requires no sensors and has no heat transfer delays to measure the internal temperature of a battery is proposed. This is based on electrochemical impedance spectroscopy measurements, where an intercept frequency relating to the internal battery temperature is determined. Mathematical analysis and experiments on various Lithium–Ion batteries conducted by the authors reveal as that the intercept frequency decreases with higher temperatures.

There is a remarkable amount of literature available on the topic of temperature measurement in Lithium–Ion batteries, with many novel methods constantly being developed and tested.

E. Thermistors

Another concept we explored towards the development of our project was thermistors. There are several papers that explore these temperature sensors, with a lot of emphasis in their resistance–temperature equations. For example, the article *NTC thermistor resistance–temperature calibration equation analysis* [17] studies seven calibration equations to see which one best agreed with the known resistance–temperature data of four different thermistors. It was found that the best equation was the Hoge–3, having an absolute error smaller than 15mK – the smallest out of all equations.

Another analysed thermistor equation is the Steinhart–Hart equation. The paper *Temperature measurement in dimensional metrology – why the Steinhart–Hart equation work so well* [18] analyses this equation that describes the electrical characteristics of an NTC thermistor, converting resistance values into temperature. To get precise and accurate conversions, the author illustrates that the full equation should be used.

More general papers about thermistors can also be observed. For example, *Properties and uses of thermistors – Thermally sensitive resistors* [19] analyses the characteristics of a thermistor. The authors use a specific thermistor with a 0.061cm diameter bead suspended in the air. As current increases, the power dissipation increases, causing an increase in temperature. Therefore, there is a decrease in resistance.

Lastly, there also is literature available on the simulation of thermistors. For example, the paper *A simple analog behavioural model for NTC thermistors inluding selfheating effect* [20] simulated the analog behaviour model of loaded and unloaded NTC thermistors for analysis of the steady–state large signal time–domain and design of NTC thermistor circuits. It has been made possible for any circuit designer to simulate a complete static current–voltage characteristic of a thermistor element using PSPICE, a circuit simulation software. The proposed NTCT ABM (analog behaviour model) and the theoretically calculated model from the manufacturer data sheet revealed that the simulation is a very good approximation.

IV. Sustainability and Risk Assessment

A. Sustainability goals

The Sustainability Development Goals are an urgent call of action by all countries, developed and developing. They consist of a list of 17 goals with the purpose to transform our world. These goals have been recognized by all United Member States in 2015 and are a priority for lots of businesses around the world when planning for future projects. Our project has been developed in a sustainable manner and directly affects on the following goals [21]:

Goal 7 – Affordable and clean energy: The MEGA-BRIC is a product that enables the use of renewable resources, encouraging the growth of affordable and clean energies.

Goal 9 – Industry innovation and Infrastructure: This project deals with innovative technologies that will mark a turning point in the energy infrastructure for underdeveloped countries.

Goal 12 – Responsible consumption and production: The MEGA-BRIC uses reusable cells, giving them a second life. Furthermore, by using renewable resources, the MEGA-BRIC can help the growth of responsible production of energy.

Goal 13 – Climate action: In recent years, climate change has begun to directly affect people's living conditions. Being a beacon of renewable energy, the MEGA-BRIC appears to be a promising solution to limiting carbon emissions. Taking this

climate action helps slow down the negative consequences of pollution, slowly remedying the impact fossil fuels have had (and are having) in our planet.

Moreover, our project indirectly affects several of the Sustainability goals, including:

Goal 1 – No poverty: The MEGA-BRIC will provide underdeveloped countries with access to electricity, taking a huge step in the fight against poverty.

Goal 3 – Good Health and Well–Being: Electricity is essential in our modern day world as it helps homes stay warm or institutions like hospitals to run properly.

Goal 4 – Quality education: The MEGA-BRIC can be used to power schools where people live in less favourable conditions.

Goal 8 – Decent work and economic growth: This project can provide economic growth to those using the MEGA-BRIC, as the expense on electricity will be reduced.

Goal 11 – Sustainable cities and communities: The MEGA-BRIC is part of the new generation of renewable energy technology that will help build sustainable cities.

B. Risk Assessment

Before starting our project, the group created a risk assessment. In order to complete it, we thought of different risks that could potentially be involved in the completion of our project. Furthermore, we established the impact this risk would have on our timeline as well as in our health. Then, the group gave each risk a parameter called "risk score", defined as the multiplication of the severity of the risk and the probability of this occurring (both out of 5). Lastly, we thought mitigating actions to minimize the probability of the risks occurring and contingency plans in case the risk actually happens. A brief summary of the risk assessment can be seen below. The full risk assessment is present in the wiki.

- **Physical injury**: While working with the BRIC there are several possible injuries that could happen. Severity = 4, Probability = 2, Risk score = 8. The mitigating action would be to follow health and safety procedures during experimentation. Depending on the severity of the injury, the contingency action would be to call emergency services.
- **Mental stress from workload**: Impact: Reduced performance and efficiency in the group project and across other modules. Furthermore, project delays and potential extension requests due to inability to complete work. Severity = 2, Probability = 4, Risk score = 8. The mitigating action would be to create a project plan that incorporates flexibility to account for additional workload. Also, meetings with supervisor will help to alleviate the stress from the workload. The contingency action would be to apply for MCF and/or request project extension as a last resort.
- **Insufficient materials**: Impact: This would create delays in the BRIC building process as well as in the testing phase. Severity = 2, Probability = 2, Risk score = 4. The mitigating action would be to count inventory at the end of each session and let Alp Technologies know about any material that might be necessary for next session. The contingency action would be to always have something else to build in case the materials for a specific part run out.
- **Equipment failure**: Impact: This would delay the project and could have a financial impact to fix the issue. Furthermore, it could lead to physical injuries. Severity = 3. Probability = 1. Risk score = 3. The mitigating action would be to inspect equipment prior to use and make sure everything works properly at the end of each session. The contingency action would be to discuss with Alp Technologies and try to find alternative equipment.

V. Objectives

As was mentioned in the introduction, the final objective of this project is to introduce temperature sensors into the BRIC to be able to monitor the temperature through each cell. In order to do this, a four-step plan was designed.

A. Step I – BRIC building

The first step towards the completion of the final product was to learn about the BRIC. This included both the circuitry of the top and bottom boards as well as assembling them. In order to do this, we

spent the first month at Alp Technologies building BRICs. We were tasked with building 20 BRICs and one analyser board, something that we achieved and gave us the basis to complete the project.

B. Step II – Experimentation

Several experiments were conducted to explore the behaviour of the BRIC and individual cells under a load. Specifically, three different experiments were designed.

C. Step III – Design

In order to complete the design of the PCB, several steps needed to be completed. Firstly, the circuitry needed to be designed, including how the temperature sensors would be connected as well as the method to read the data.

Once the specific circuitry was known, the components that were going to be in the PCB had to be chosen. This included the choice of temperature sensors, resistors, ADCs and analyser board.

Knowing the components we were going to use, we were then ready to start the schematic design in Altium. This part was simply mapping the designed circuitry to a schematic in the PCB editing software.

Also, the PCB itself needed to be designed. In order to do this, we had to place all the footprints in the PCB in an efficient manner and correctly connect all of the components together, be it with filled zones or traces.

Lastly, the code had to be created to interact with the new design of the board. This code was produced in Arduino and interacted with the ESP32 to obtain the temperatures of each cell.

D. Step IV – Testing and Analysis

The last step in our four-step plan was to test the PCB to make sure it responded as intended. This included making sure we were able to read the different temperatures from all the sensors as well as making sure the read data corresponded to the correct temperature.

E. Research

As we were completing the four aforementioned steps, a literature review was done in tandem to give us an understanding of the theory behind everything we were doing, as well as to provide an insight into current developments in the field.

VI. Step I – BRIC building

As was mentioned earlier, the first step in our four–step plan was to build 20 BRICs and one analyser board. BRIC building is a three step process: Firstly, the components have to be soldered onto the top and bottom boards, to then finally assemble the BRIC together.

A. Soldering the Top Board

Unlike the bottom board, the top board has two sides with components soldered onto them. The top side of this board is quite simple, all that needs to be done is add the fuse wire. To do this, the whole length of wire is soldered. It is important that it is tight and along the entire row of fuses, as when the solder paste is applied, the wire has to stick between its connections. When the board had finished its period in the soldering oven, the fuse wire has to be cut so only the fuse connections are left in place. At this moment, we analyse the top side of the top board. If there are any fuse connections that have not soldered correctly, they have to be soldered manually. Fig. 3 shows the top side of the top board with the fuse wire soldered onto it.

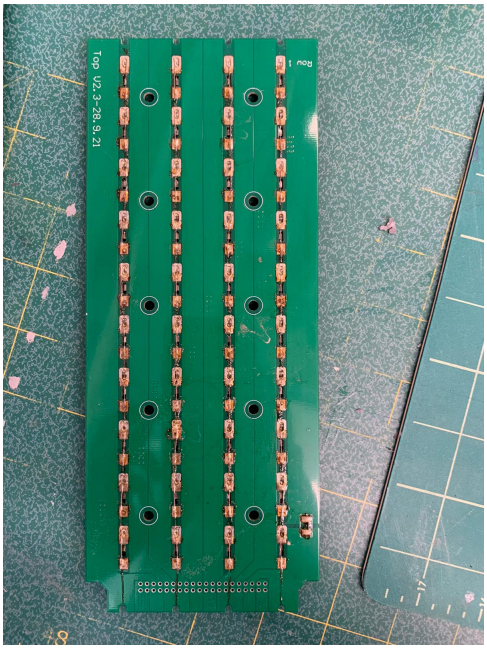

Fig. 3: Top side of the top board

With the top side completed, we can move on to soldering the bottom side. This is a two step process. Firstly, the spring clips have to be soldered

using solder paste and the re–flow oven. Then, the connector for the ribbon cable has to be manually soldered. With this done, the top PCB is ready.

B. Soldering the Bottom Board

The bottom board only has one side that has to be soldered, making it simpler than the top PCB. For this board – unlike the top PCB – only the spring clips have to be soldered with the re–flow oven. With these soldered in, several items have to be soldered by hand, including the connector for the ribbon cable, the header for the Analyser board and a third connector in case the desired system is a 4–BRIC–1–analyser–board module.

With everything soldered in the bottom board, the rivets have to be added. These fasteners are applied through the use of a hand riveter. Fig. 4 shows a bottom board with the spring clips and rivets, as well as the three locations for the connectors that have to be manually soldered.

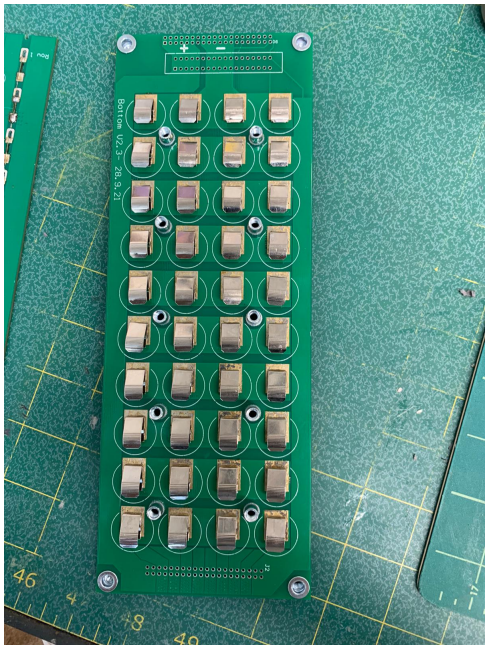

Fig. 4: Bottom board of the BRIC

C. Assembling the BRIC

With both the top and bottom boards soldered, there are several steps to complete in order to have an assembled BRIC. First of all, the ribbon cable has to be created. This is done by attaching two connectors to a set of joint wires that connect the two boards. In this step it is very important to take into account the direction of the connectors, as if the ribbon cable is created the wrong way, the two PCBs are not going to be able to connect to each other.

With the ribbon cable done, the 40 cells that are going to be in the BRIC need to be placed into the cell holders. This is quite simple to do, the only concern is to make sure the orientation of the cells is constant across the 40 of them.

Once this is ready, the BRIC can be assembled and bolts can be inserted between the top and bottom boards to secure everything together. The next step, is to use a special tool – two 3D-printed legs connected together, separated by the BRIC's desired height – to measure whether or not the distance between the two boards is correct. Finally, four 3D-printed legs are screwed into the BRIC such that it is not laying on the bottom PCB. Fig. 5 shows four assembled BRICs in the 4–BRIC–1–analyser–board configuration.

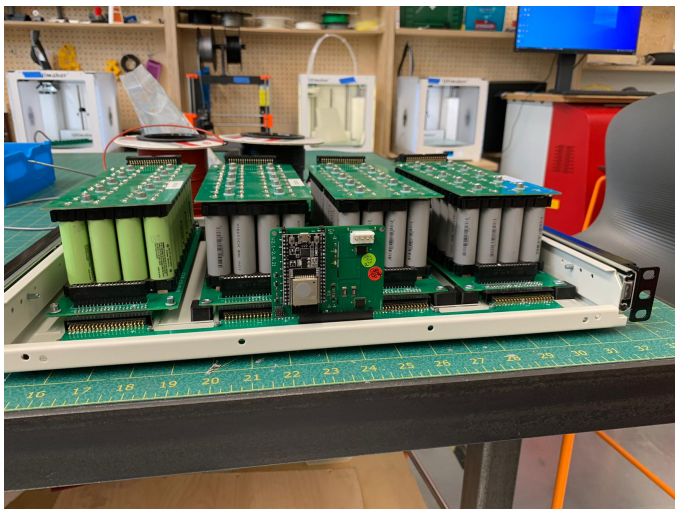

Fig. 5: 4-BRIC Configuration

D. Discussion

While originally tasked with building 20 BRICs, due to time constraints we were only able to finish 18 of them. Still, the experience of building that amount of BRICs gave the group a deep understanding of the functioning of the battery as well as the design that was integrated to build it. This experience would then help us with the design of our

own PCB as well as a more efficient construction to conduct the testing.

VII. Step II – Experimentation

Before starting to design the PCB, three separate experiments were conducted to explore how temperature fluctuates both within an individual cell and the BRIC as a whole.

A. Experiment I – BRIC temperature at low current

1) Methodology: The first experiment performed was intended to show whether Lithium–Ion cells indeed do increase temperature inside the BRIC when running a current through them. Furthermore, if it can be confirmed that the temperature does increase, it would be interesting to know by how much it increases to help decide at what temperature our future code will flag. Moreover, the experiment was performed twice, once with new cells and a second time with recycled cells in order to see the difference in performance between them.

For this experiment, the circuit in Fig. 6 was used.

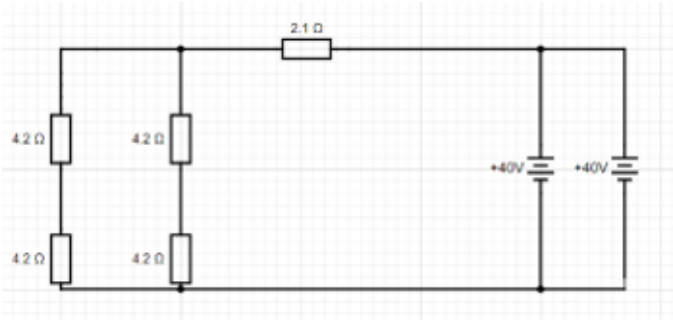

Fig. 6: Circuit used for Experiment I[4]

The equivalent resistance can be evaluated to,

$$R_{NET} = \left(\frac{1}{4.2+4.2} + \frac{1}{4.2+4.2}\right)^{-1} + 2.1 = 6.3\Omega \quad (1)$$

Then the total current can be found,

$$I_{NET} = \frac{40}{6.3} \simeq 6.349A \quad (2)$$

Finally, since the BRICs have equal voltages, the current splits evenly among them,

$$I_{BRIC} = \frac{6.349}{2} = 3.1745A \quad (3)$$

[4]Author's own using circuit design software [22]

This specific circuit had to be used due to power and voltage issues through the BRIC and resistors. First of all, the 4.2Ω resistors have a limiting voltage of $24V$, therefore it's not possible to simply connect one of these directly to a BRIC. Furthermore, the two BRICs in parallel are used to control the current through each BRIC. In practice, the current through each BRIC should not surpass $5A$, therefore this was replicated in the experiment.

Once the circuit was built, a FLIR ONE Pro thermal imaging camera attached to an iPhone was used to measure the temperature through the cells. The BRIC was left running for 90 minutes, with constant monitoring of the temperature of the middle rows with the thermal camera. After the 90 minutes, the BRIC was quickly opened to attempt to see the temperature distribution inside the BRIC. Fig. 7 shows Experiment I as we configured it.

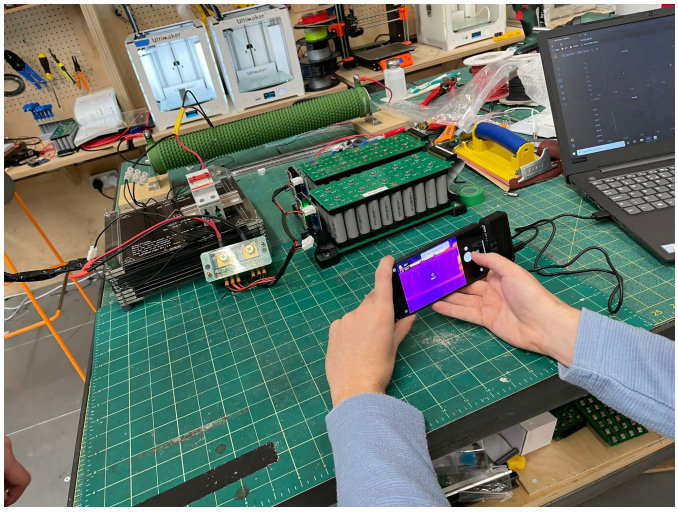

Fig. 7: Experiment I Real-life Configuration

2) Results: As was mentioned earlier, Experiment I's objective was to explore the heating curve of cells under a load. Mainly, we wanted to find out whether cells heated up under a load. Furthermore, if they did heat up, it would be interesting to see how big this increase is. Lastly, we wanted to compare this possible increase in temperature between new and used cells.

The main hypothesis for this experiment was that new cells would not heat up, or, if they did, the temperature increase would be minimum. On the other hand we believed that recycled cells would heat up more due to cell degradation. The more

a cell is used, the more degraded it is, therefore the higher its internal resistance and the higher the power dissipation through it is. This results in a higher cell temperature.

Table II and Fig. 8 show the results for this experiment.

TABLE II: Data for Experiment I

Time(mins)	**Temperature**(°C)	
	New Cells	***Recycled Cells***
0	24.1	25.7
12.5	24.5	26.2
25	24.8	26.9
37.5	25.6	27.7
50	25.3	28.8
62.5	26.1	29.6
75	25.8	30.0
90	26.4	30.7

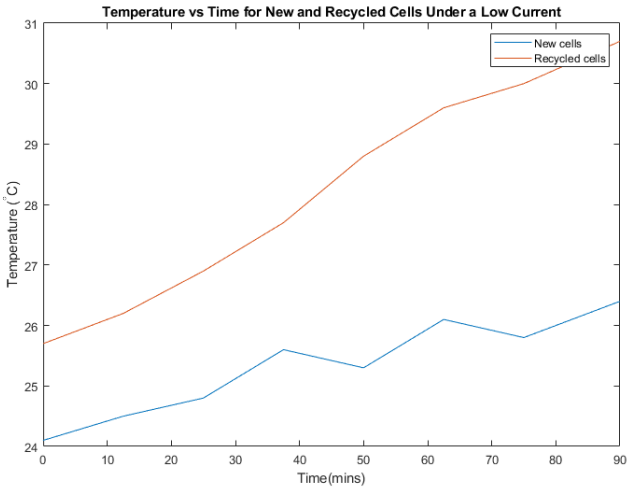

Fig. 8: Results of Experiment I

3) Discussion: The data in the above table shows several concepts. First of all, it demonstrates that cells, even new ones, indeed do heat up under a load. This is evidenced by the, albeit small, increase in cell temperature.

Furthermore, recycled cells did in fact heat up more than the new ones, which was expected.

As can be seen in Fig. 8, there is a clear correlation between cell temperature and time for both new and recycled cells, with the recycled cells having a steeper gradient. It is important to mention that the figure shows that recycled cells had a higher starting temperature than new ones. This is due to the tolerance of the camera, which, when researched on the website, can be seen to be ±5% [23].

This Experiment gave the group a good initial understanding of the behaviour of the BRIC under a small load. With this baseline information, we could then go on to design more specific experiments to explore different characteristics of the BRIC, or explore BRIC behaviour under different circumstances.

B. Experiment II – temperature through individual cells

1) Methodology: The second experiment was designed to show temperature fluctuations in individual cells at high currents. In order to do this, a cell was placed in a cell holder designed by Alp Technologies and connected to a variable resistor[5]. The discharge current was then increased to 10A and the cell temperature was measured using the same thermal camera as in the first experiment. Fig. 9 shows the discharging cell as seen by the thermal camera.

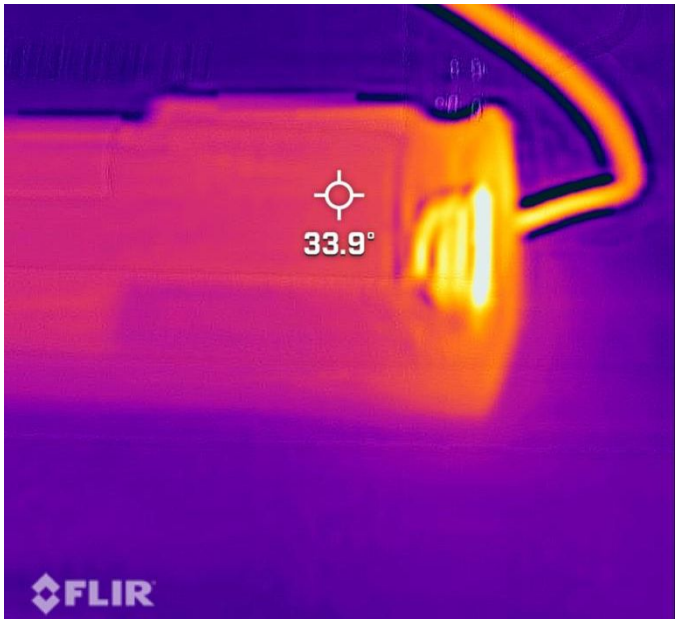

Fig. 9: Experiment II as Seen by the Thermal Camera

[5]The exact model is the DS09025R12UP024

Since the final goal is to use the BRIC with recycled cells, these were used in the experiment. Specifically, two different cell brands were used: Panasonic and Samsung.

Furthermore, to explore where in the cell the biggest temperature increase occurs, the temperature at both the anode and cathode was measured.

2) Results: In this experiment, a much higher current was run through individual cells to emulate a potential issue with the BRIC or a situation in which it might be desirable to have a bigger current than the specified limit of 5A is needed.

The formula for power dissipation is,

$$P = I^2R \tag{4}$$

Therefore, with the same internal resistance, a cell will dissipate more power if a bigger current is run through it, resulting in a bigger increase in temperature. Because of this, the hypothesis for this experiment was that cell temperature would be substantially higher than in Experiment I.

The experiment results for the Panasonic cell can be seen in Table III and Fig. 10:

TABLE III: Data for Experiment II – Panasonic Cell

Time(s)	**Temperature**(°C)	
	Anode	***Cathode***
0	25.5	25.5
15	26.2	32.3
30	27.8	41.1
45	29.1	48.8
60	30.5	57.1
75	31.3	61.9
90	32.8	67.1
105	34.0	68.5
120	35.7	72.4
135	36.8	75.3
150	38.6	76.7
165	40.3	82.7
180	42.4	85.6

On the other hand, data for the Samsung cell can be seen in Table IV and Fig. 11.

3) Discussion: As can be seen in the tables, the first noticeable concept is that the temperature increases to a much higher quantity than in the first experiment, with some cells reaching 85°. Furthermore, there was a big difference in temperature between Anode and Cathode in both cells. The main takeaway from this experiment relates to sensor

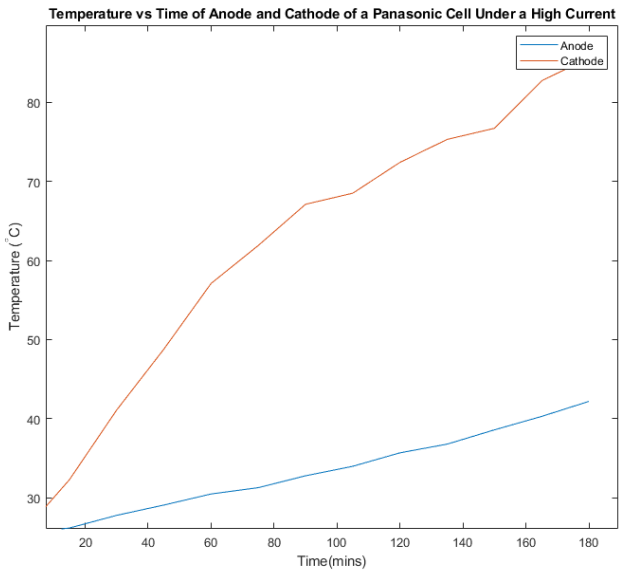

Fig. 10: Temperature vs Time of Anode and Cathode of a Panasonic Cell Under a High Current

TABLE IV: Data for Experiment II – Samsung Cell

Time(s)	**Temperature**(°C)	
	Anode	***Cathode***
0	25.6	25.6
15	26.1	36.2
30	27.0	43.6
45	27.7	50.1
60	28.4	55.3
75	29.1	57.2
90	30.0	62.9
105	31.4	63.3
120	32.6	62.9
135	33.3	63.6
150	34.2	64.1
165	35.9	62.7
180	36.7	63.0

placement within the BRIC. We now know that the cathode reaches a much higher temperature than the anode, therefore the highest temperature change can be observed in the bottom section of the BRIC. For this reason, we decided to place the temperature sensors on the bottom PCB.

C. Experiment III – BRIC temperature at higher currents

1) Methodology: As can be seen in Fig. 12, while performing the first experiment, the ribbon cable that connects the top and bottom PCB got very warm, achieving a temperature of 61.7°C.

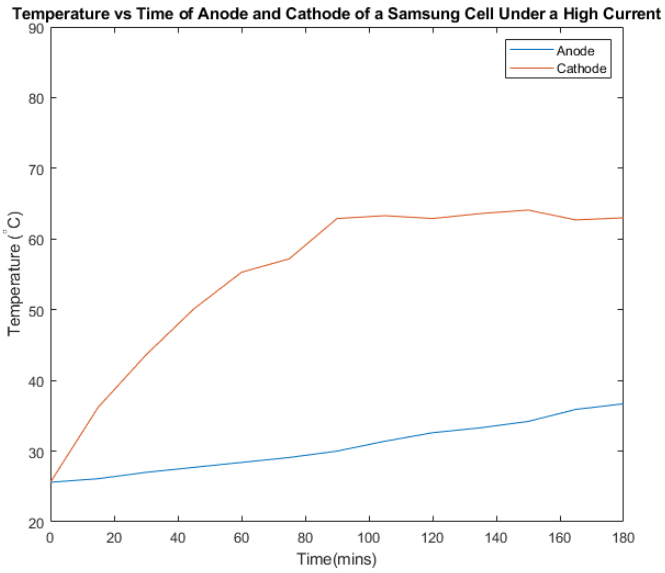

Fig. 11: Temperature vs Time of Anode and Cathode of a Samsung Cell Under a High Current

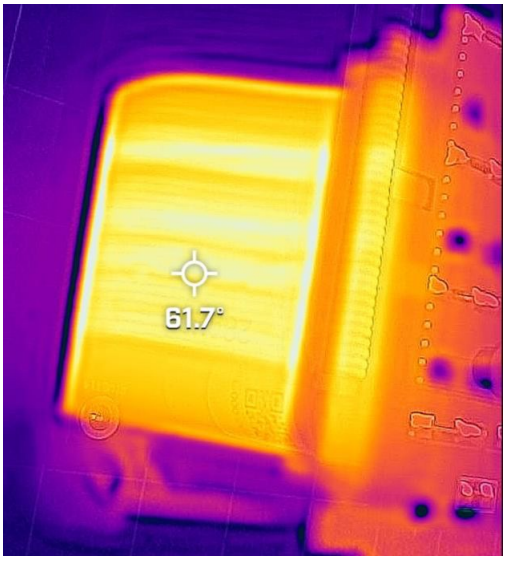

Fig. 12: Ribbon Cable During Experiment I

Because of this, a third experiment was designed to see how this affects the general temperature of the BRIC. A similar circuit was used as in the first experiment, but using one BRIC instead of two. The circuit can be seen in Fig. 13.

Using the same method as for experiment I, the current through the BRIC can be evaluated to,

$$I_{\text{BRIC}} = 6.349A \tag{5}$$

Just like with Experiment I, the BRIC was left

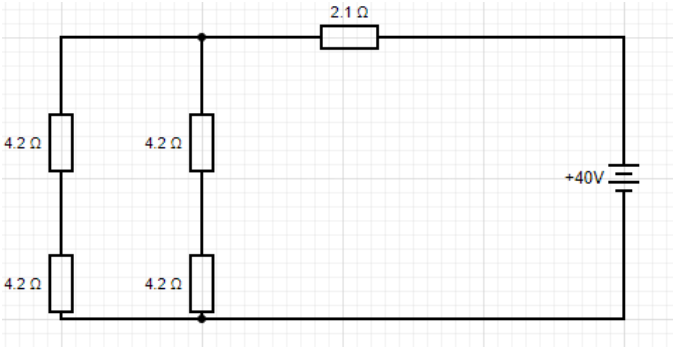

Fig. 13: Circuit used for Experiment III

running for 90 minutes, and the temperature of both the cells and the ribbon cable was measured with the same thermal camera connected to an iPhone. Unlike the first experiment – where the temperature was only monitored in the middle of the BRIC – in this experiment the temperature of every row was measured. After 90 minutes, the BRIC was opened to observe the temperature distribution throughout the 40 cells. Just like in the second experiment, temperatures were measured at both the anode and cathode of the cell.

2) Results: Table V shows cell temperature by row number in the BRIC. Note that row 1 is the row furthest away from the ribbon cable, and row 10 is the closest one to it.

Furthermore, Fig. 14 shows a bar chart with row temperature per row for both the anode and cathode of the cells.

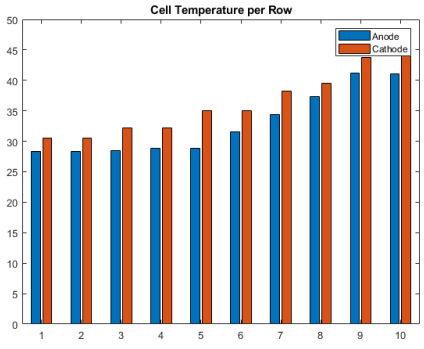

Fig. 14: Cell Temperature By Row in Experiment III

3) Discussion: As can be seen in the above table and figure, there is a clear temperature increase as the cells get closer to the ribbon cable. This is

TABLE V: Data for Experiment III – Row temperatures

Row number	Temperature(°C)	
	Anode	***Cathode***
1	28.4	30.5
2	28.4	30.5
3	28.5	32.2
4	28.9	32.2
5	28.9	35.0
6	31.6	35.0
7	34.4	38.3
8	35.7	39.5
9	37.6	41.6
10	38.8	42.8

an important concept to take into account when deciding what temperature to set the flag at, as different cells within the BRIC are at different temperatures.

VIII. Step III – Design

A. Design choice

The first item in the agenda towards completing the final product was to choose our design. This mainly consisted on deciding on the number of sensors present in the BRIC and where within it they would be placed.

As was mentioned earlier, Experiment II showed that the part of the cell that shows the biggest increase in temperature under a load is the cathode. Because of this, we decided to place the sensors in the bottom PCB of the BRIC, closer to the cathode.

In terms of the number of sensors present, there were two main designs that could be used, trading precision in the temperature measurements for a more cost-effective design. The first alternative was to have 40 sensors, one for each cell, as can be seen in Fig. 15. In the figure, the horizontal lines represent temperature sensors and the circles represent cells.

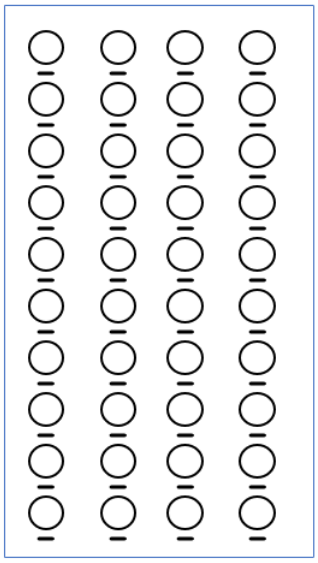

Fig. 15: First design option - 40 sensors

This design would provide the most accurate readings as each cell had an accompanying sensor, giving the exact temperature[6]. One problem with this design was that it would require the purchase of 40 sensors and 40 resistors[7] per PCB, resulting in a higher cost.

The second design option was to have one sensor every four cells as shown in Fig. 16.

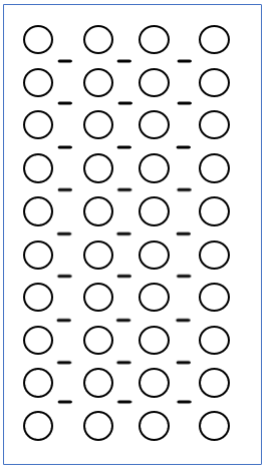

Fig. 16: Second design option - 27 sensors

[6]An important assumption here is that the sensors measure cell temperature rather than ambient temperature within the BRIC

[7]For every sensor present there has to be a resistor accompanying it. This will be further explained later

This summed to a total of 27 sensors, 13 less than in the first design. While less accurate, this resulted in a lower production cost, an element that also has to be taken into account. The rationale behind this design stemmed from the fact that knowing the exact temperature of every cell was not absolutely necessary. Given there was a faulty cell, its temperature would substantially increase. Therefore we really were only concerned with temperature increases rather than the actual value. In the case that there was a faulty cell that was at a higher temperature, depending on what sensors picked up this increase, one could localize the exact cell that was causing the issues. There were three possible scenarios that could happen:

1) A corner cell is the faulty one: In this case, only the sensor closest to it will show this increase in temperature
2) An edge cell is the faulty one: In this case, only the two sensors closest to it will show the increase in temperature
3) A middle cell is the faulty one: In this case, the four sensors in each corner of the cell will show the increase in temperature

Examples of these three situations can be seen in Figs. 17–19. In these images, the faulty cell is shown in red and the sensors showing the increase in temperature are shown in blue[8].

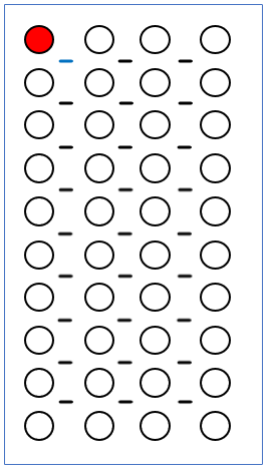

Fig. 17: Case I - The faulty cell is in a corner

After much deliberation, we decided to have both designs available in the PCB, and Alp Technologies would decide which one they would use when soldering it. This was quite simple to enact and will be further explained in the following subsections.

[8]All three figures were created by the author in PowerPoint.

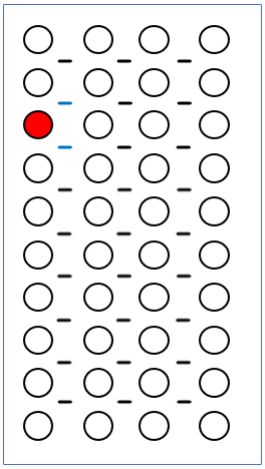

Fig. 18: Case II - The faulty cell is in an edge

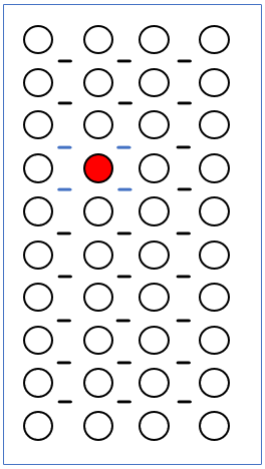

Fig. 19: Case III - The faulty cell is in the middle

B. Choosing the Sensor

Before moving on to the circuit design, we needed to decide what type of temperature sensor we would use in the PCB. Different types of sensors are connected in different ways, therefore we couldn't design the circuit without knowing what sensor we would be using.

There are several types of temperature sensors, including thermocouples, resistance temperature detectors (RTD) or thermistors, all of which come with their advantages and disadvantages. One big concern in our project is budget, as our final design

has to be affordable for Alp Technologies. Because of this, RTDs were discarded from the choice, as they tend to be more expensive than thermocouples and thermistors.

Furthermore, one disadvantage of thermocouples is that they require precise amplification due to the small signal they produce resulting in an added cost in our design [24].

As was mentioned earlier, in order for us to be able to identify a faulty cell, we do not require an accurate measurement of every cell, but rather we need to observe significant changes relative to other cells. For this reason, we decided to use thermistors as our measuring device. While not always accurate, they are sufficient if our goal is to identify relatively big changes in temperatures of individual cells.

Thermistors come in two types: Negative Temperature Coefficient (NTC) and Positive Temperature Coefficient (PTC). The main difference between these two is the relationship between its resistance and the temperature. In NTCs, resistance decreases with an increase in temperature. The opposite occurs in PTCs, where resistance increases with an increase in temperature. Fig. 20 shows a typical response for NTC and PTC thermistors [25].

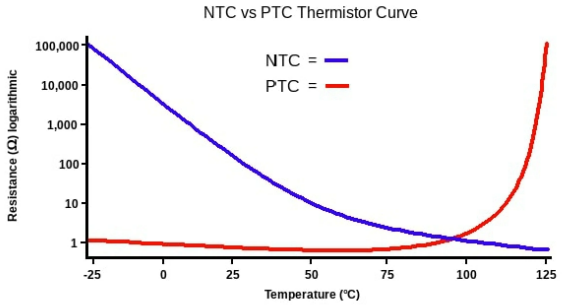

Fig. 20: Typical response for NTC and PTC thermistors

Usually, PTC thermistors are used as current-limiting devices, acting as a replacement for fuses. On the other hand, NTC thermistors are more generally used to monitor temperature. The reason why this is the case can be seen in Fig. 20, which showcases the Resistance–Temperature relationship of these two types. Since PTCs only experience a significant change in resistance at high temperatures, they would not be suitable for our purpose. Because of this, we decided to choose an NTC model instead as it would allow us to monitor resistance changes at a broader range of temperatures. With that in mind, we selected the **ERTJ1VT102H** NTC thermistor. As can be seen in its datasheet[9], one of its recommended applications is temperature detection of cells within a battery pack [26].

C. Circuit Design

Once the general design and the specific sensor we would use were known, the next step towards the completion of the new PCB was to design the circuitry. The simplest way to use a thermistor to measure temperature is through a simple voltage divider circuit. Fig. 21 shows a simple design of how the circuit would look like for one cell, where the value of the power source and the resistor will be chosen later based on the choice of the thermistor.

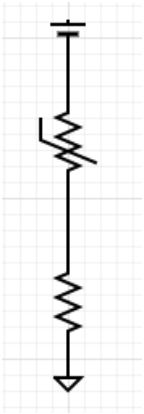

Fig. 21: Circuitry for a single thermistor

By taking the output voltage between the output voltage between the sensor and resistor, the thermistor resistance can be obtained:

$$R_t = \frac{V_s}{V_{out}} \cdot R_r - R_r \tag{6}$$

Where R_t is the thermistor resistance, V_s is supply voltage, V_{out} is output voltage and R_r is resistor resistance. Once the thermistor resistance is known, the corresponding temperature can be obtained by looking at the given table in the datasheet.

With this in mind, the circuitry to implement this as to have one sensor per cell is by replicating this

[9]Datasheets for all components available at [28]

design 40 times in a 4p10s configuration, similarly to the BRIC. On the other hand, if the chosen design is the one with 27 thermistors, the above design has to be replicated that number of times in a 3p9s configuration, as seen in Fig. 16.

As it was mentioned earlier, the aim was to have the board with footprints in order to be able to implement both designs. Meaning that when soldering the sensors in Alp Technologies, we could choose which one to use. The problem is that, for this to happen, the PCB would need to have 67 footprints and wires. This is an issue because it is generally not a good idea to overcrowd a PCB with wires. An elegant solution to avoid this problem stems from the fact that in any given PCB, the sensors will be placed either in one configuration or in the other, never both simultaneously. Because of this, two sensors are able to share one same wire, as long as both thermistors belong to different configurations. Using this, there can be 67 footprints for all of the sensors, but only 40 wires.

After designing the sensor circuitry, the next step is to find a way to read the voltage through each thermistor. Since Alp Technologies includes an ESP32 in their analyser board, we decided to use an ESP32 as well to simplify future implementation for the company.

The ESP32 has 16 built–in ADC inputs, while our design has a maximum of 40 input lines. Because of this, we decided to use an external ADC. Even when using an external ADC, this still results in 40 inputs, while the ESP32 has a maximum of 32 GPIO pins. Therefore, in order to connect these ADCs to the ESP32, we had to use the I^2C protocol. Another advantage of using I^2C is that we can minimize the number of wires we use, as we can connect the outputs of the ADCs together in a master–multiple slaves configuration.

D. Choosing the components

Once the thermistors were chosen and knowing the circuit we would use, we were able to choose the resistors that would be connected in the voltage divider circuit. Since the chosen thermistors have a room temperature resistance of 1kΩ, we decided to match them with the resistors and chose a resistance of 1kΩ[10] for simplicity in future calculations.

The next component to specify were the Analog–to–Digital Converters. The first factor to consider was the number of channels they would have. ADCs come in a range of channels, commonly varying from one to sixteen. The most efficient choice was to choose an 8-channel ADC, as that would leave us with no excess channels.

As was mentioned earlier, we aimed to use the I^2C protocol for communication between the ESP32 and the ADCs. Therefore for our circuit we needed an 8-channel ADC that allowed for I^2C communication. One component that matches these requirements is the **NCD9830 8-bit, 8-channel ADC with I^2C Serial Interface**[11].

Looking at the datasheet for the ADC, it can be seen that it can have one of four I^2C addresses. Because of this, we could not have all five of them connected together to the same bus. Thankfully, the ESP32 can support two different I^2C buses; we can then remedy this issue by connecting three ADCs to one of the buses and the remaining two to the other one. The datasheet also recommends connecting the ADCs to power via a 10μF capacitor[12] in order to reduce the noise. This was replicated in our circuit.

E. Schematic Design

Once the exact components we were going to use and the circuitry that would be implemented were known, designing the schematic was a matter of replicating the circuit in Altium. Fig. 22 shows the Altium schematic for the first two rows of thermistors and resistors. It can clearly be seen how two resistors from different configurations share a wire.

Figs. 23 shows the connections for the ADCs. Pins SDA and SCL belong to the I^2C bus. Furthermore, pins A0 and A1 are the I^2C address pins and their value is assigned by connecting them to either HIGH voltage or to ground. Since there are two pins, this leads to a total of four possible addresses. As

[10]Specific component is CR0402AFX–1001GLF https://www.mouser.co.uk/datasheet/2/54/cr_a-1858337.pdf

[11]Specific component is NCD9830DBR2G https://www.onsemi.com/pdf/datasheet/ncd9830-d.pdf

[12]Specific component is the C0805C104K5RAC7411 https://www.mouser.co.uk/datasheet/2/212/KEM_C1002_X7R_SMD-1102033.pdf

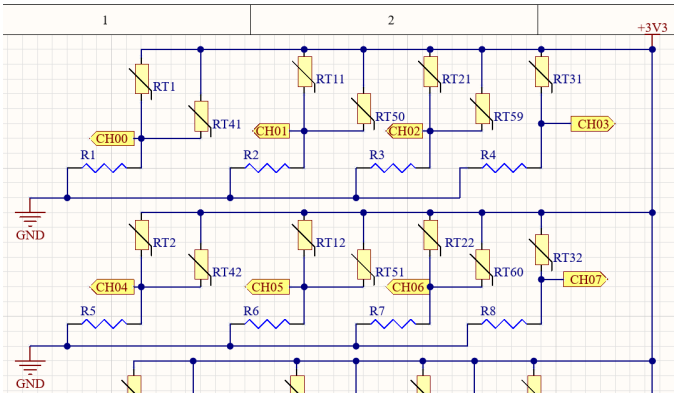

Fig. 22: Circuit schematic for 2 rows of the PCB

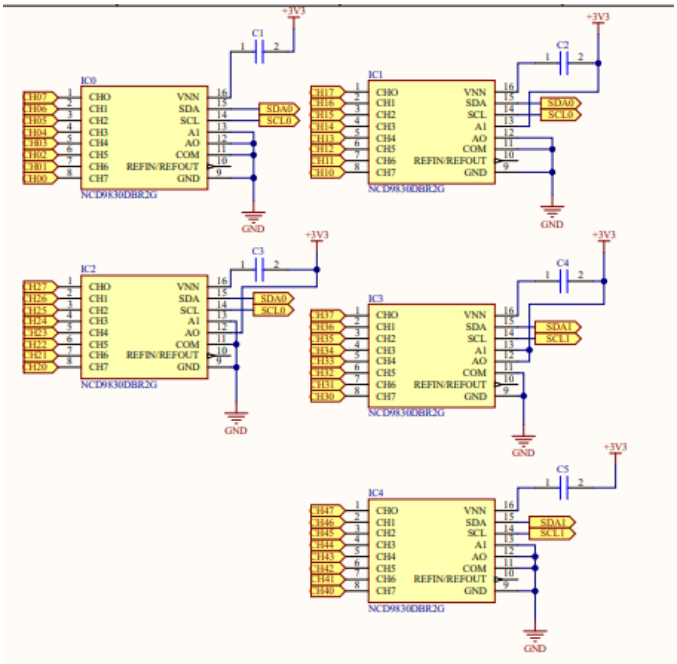

Fig. 23: ADC connections

TABLE VI: ADC addresses

ADC	A0	A1	Hex
0	0	0	0x48
1	0	1	0x4A
2	1	0	0x49
3	1	1	0x4B
4	0	0	0x48

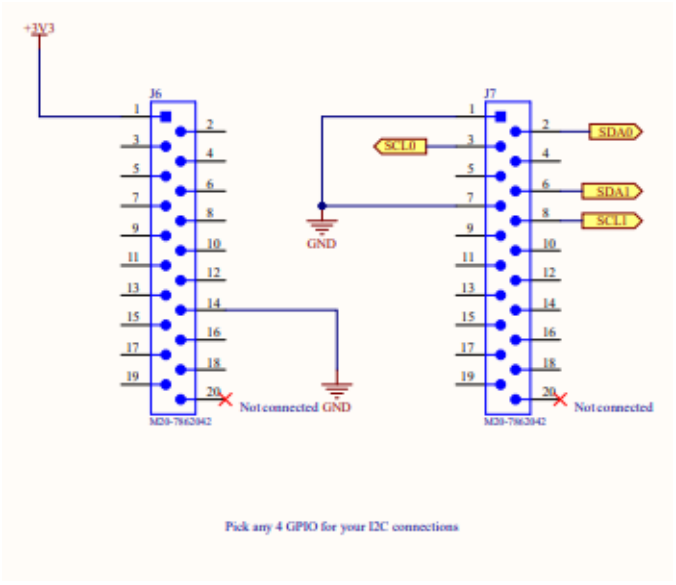

Fig. 24: ESP32 header connections

we had five ADCs, this led us to have to use two separate I^2C buses.

Table. VI shows the different addresses for the different ADCs. Note that two ADCs share the same address, but this is not an issue since they are connected to the ESP through separate I^2C buses.

Lastly, as per recommendation from the ADC producers, a capacitor is added between the VDD pin and supply voltage in order to reduce noise.

Fig. 24 shows the connections for the ESP headers, and Fig. 32 in Appendix D shows the entire schematic .

F. PCB Design

In order to be able to accommodate both possible configurations on our board, we had to significantly modify the design of the BRIC's PCB. Space constraints were one of the main challenges involved with creating our version of the bottom board. Currently, ALP Technologies uses a 2–layer design in which both planes include a fill zone on nearly their entire area, leaving little room for any additional components. Fig. 25 shows Alp Technologies' original bottom board design.

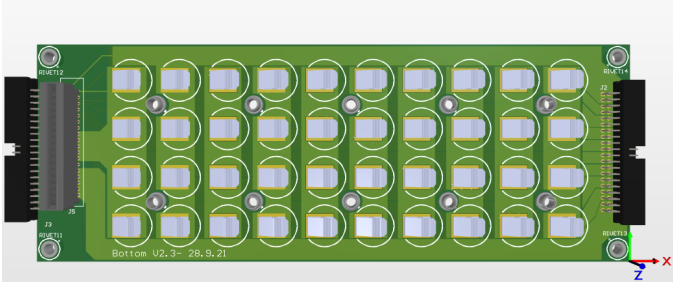

Fig. 25: Alp's original bottom board design

The first thing to modify was adding two additional middle layers to the board. This allowed us to have room to include two new fill zones for ground (GND) and voltage supply (+3.3V) on a layer of their own. This solution allowed us to fit every component required and minimise the amount of tracing.

The next step was adding the thermistors and resistors to the board. In order to be able to do that we had to modify the fill zones present on the top layer, by making cutouts for every thermistor.

Power and ground would be delivered from the two mid-layers to the top-layer by using through–hole vias. Each thermistor makes a connection with 2 vias, one connecting it to +3.3V, while the other is the intersection between the thermistor, resistor (the second terminal runs to GND also through a via) and the ADC. The figure below shows an example of how these connections are traced on the board. Red represents copper present on the top layer, brown on the 1st mid-layer (GND plane) and light blue on the 2nd mid-layer (+3.3V plane). Moreover, in most cases a second thermistor also connects to the latter via the track highlighted in white on Fig. 26. These are the thermistors which would be used in the second configuration.

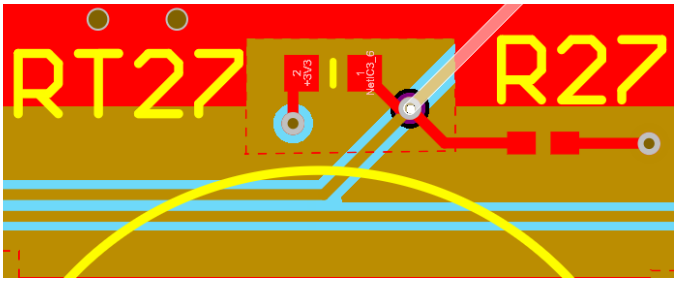

Fig. 26: Thermistor connections

In order to be able to fit the larger components (ADCs and ESP32 headers), the board had to be widened.

By taking advantage of the I^2C protocol, we reduced the amount of connections between the ADCs and the ESP32. I^2C buses require two connections, one for the data line and another for the clock line. In our design, we decided to have three ADCs use one common bus and the other two use another. Thanks to this method we do not need each thermistor value to be recorded in a separate input of the ESP, which would be impossible. Instead, every connection is made using 4 wires (2 per bus).

Except the four aforementioned wires to the ADCs, the ESP32 also connects directly to a ground fill zone on the top layer under the headers. We have added multiple vias which connect this fill zone to the one on the first mid–layer, which is how ground is distributed to the entire board. The ESP32 also supplies the 3.3V through a track and a via going to the second mid–layer.

We have decided to place the majority of the tracks on the same layer as the GND fill zone. This made routing simpler as we had the entire area of the board to place our traces on.

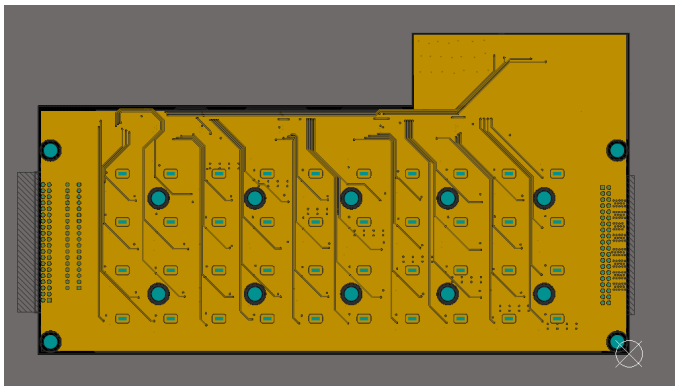

Fig. 27: Mid layer 1 - GND plane and traces

On Fig. 27 you can see the GND plane which goes to the entire board, providing every component with a common ground. On the other hand, Fig. 28 shows the voltage supply plane, which provides 3.3V to the thermistors and ADCs. This is powered through the ESP32 voltage output terminal.

Lastly, Fig. 29 shows the final 3D view of our design.

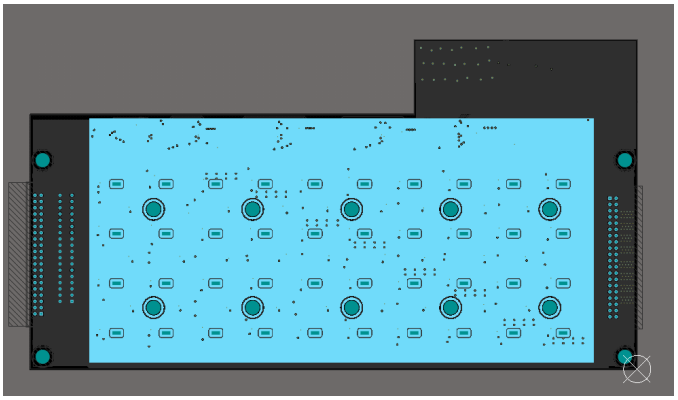

Fig. 28: Mid layer 2 - +3.3V plane

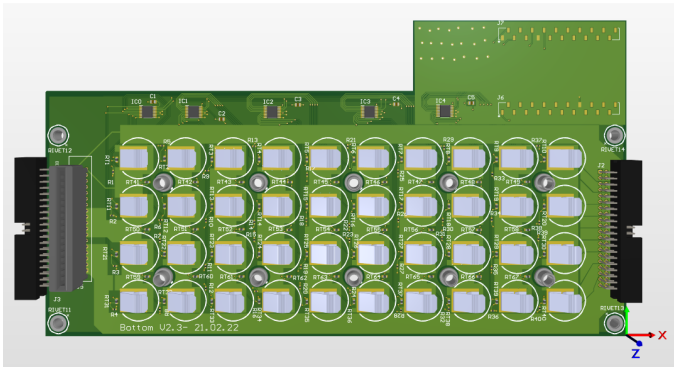

Fig. 29: Our design

G. Designing the code

In order to test the design, we must first create the code to read the output from each thermistor. This was accomplished using the Arduino IDE. Since the ADCs use the I^2C protocol, we used the **Wire** library. In the code, we created an 10x4 array which contains the received digital output from the channels of the ADCs. Reading the output is accomplished by first establishing a connection to an ADC address with *Wire.beginTransmission()* and writing to the required channel with *Wire.write()*. We end transmission to the device with *Wire.endTransmission()* after reading the channel output via *Wire.read()*. In order to transform said output to the thermistor resistance, we started with the potential divider equation for the output voltage V_O:

$$V_O = V_S \cdot \frac{R_0}{R_{th} + R_0} \tag{7}$$

where R_0 is the resistance of the resistor, and V_S is the voltage supplied to the thermistor of resistance R_{th}. Rearranging for R_{th} we find

$$R_{th} = R_0 \left(V_S \left(\frac{1}{V_O} \right) - 1 \right) \tag{8}$$

We also noted the relation between V_O and its corresponding digital output ADC_{VAL} from the ADCs. Given the reference voltage V_{REF} and maximum ADC value ADC_{MAX}[13],

$$\frac{ADC_{MAX}}{ADC_{VAL}} = \frac{V_{REF}}{V_O} \tag{9}$$

Substituting V_O from (10) into (9), we arrived at an equation for the thermistor resistance:

$$R_{th} = R_0 \left(V_S \left(\frac{ADC_{MAX}}{V_{REF} \cdot ADC_{VAL}} \right) - 1 \right) \tag{10}$$

With the resistances of each thermistor obtained, we can either find the corresponding temperature via a look-up table available in the sensor datasheet or perform further calculations. The beta constant β is a value that relates these two variables and can be used to approximate the response curve of the component over a range of temperature values. This value is generally supplied by the manufacturer, but can be obtained through experimentation via the equation

$$\beta = \frac{\ln \frac{R_{T1}}{R_{T2}}}{\frac{1}{T_1} - \frac{1}{T_2}} \tag{11}$$

This is then rearranged for T_2, resulting in

$$\frac{1}{T_2} = \frac{1}{T_1} + \frac{1}{\beta} \ln \left(\frac{R_{T2}}{R_{T1}} \right) \tag{12}$$

Two data points are required to find β, with R_{T1} and T_1 being the resistance and temperature at data point 1, and R_{T2} and T_2 being the resistance and temperature at data point 2. The temperatures (and beta) are in kelvins, whereas the resistances are in ohms.

The nominal resistance of the chosen thermistor is 1kΩ at standard temperature (25°C = 298.15K). We can substitute this values as data point 1 to calculate the temperature T for any given measured resistance.

$$\frac{1}{T} = \frac{1}{298.15} + \frac{1}{\beta} \ln \left(\frac{R_{th}}{1000} \right) \tag{13}$$

[13]The internal reference voltage of the 8-bit NCD9830 was used for this circuit: V_{REF} = 2.5V. $ADC_{MAX} = 2^8 - 1 = 255$.

IX. Step IV – Testing the Design

With the design completed, the components and PCB design were ordered to a provider. Once everything arrived, four BRICs were assembled with our new design of the bottom board. Two BRICs were soldered with the 40–sensors design, while the other two were made to have 27 sensors.

To our great dismay, when we tried to read the ADC outputs from the ESP32, we realized this could not be done. There are several theories as to why this happened, ranging from communication issues between the ESP32 and the ADC components to an underlying fault in the code implementation. While we were unable to read the digital values, there still was an input voltage into the ADCs. Because of this, we decided to separately test the PCB and the code. In order to test the PCB, we used a digital multimeter to measure the input voltage into all of the ADC channels. From those voltages, the thermistor resistance and temperature can be measured using the aforementioned methods.

To test the PCB, we replicated the previously mentioned experiments I and III. Due to time constraints, we were unable to test the 27–sensors design and could only test the one–sensor–per–cell PCB.

A. Replicating Experiment I

In order to replicate the first experiment, we connected the BRIC to the same circuit as in the experiment. In Experiment I only the temperature of the middle rows was measured, so we replicated this in the testing phase by measuring the voltages of the middle rows only. Furthermore, the temperatures were also monitored using the same thermal camera. Table. XII in Appendix B-A shows the average voltage of the fifth and sixth row in the BRIC with respect to time. Through simple mathematical manipulation and using the lookup table in the thermistor datasheet, the equivalent temperatures can be obtained. These can be seen in Table. VII.

We can compare these results obtained with the data from the thermal camera in Table VIII.

B. Replicating Experiment III

To replicate Experiment III, the same circuit was constructed. Then, the input voltages into each channel of the ADC were measured. Furthermore, the temperature of every outside cell was monitored. Table. XIII in Appendix C-A shows the voltages for all 40 thermistors after 90 minutes. This table is intended to replicate the thermistor configuration, where the first row is the row furthest away from the ribbon cable. From these results, the average row voltage can be obtained. From there, the average row temperature can be seen in Table. IX.

This can be compared to the results obtained with the thermal camera in Table X. This only shows the row averages and the full data can be seen in Table. XIV in Appendix C-B.

TABLE VII: Temperature vs Time - rows 5 & 6

Time (minutes)	Average Temperature (C°)
0	25
15	26
30	27
75	29
90	32

TABLE VIII: Temperature vs Time - rows 5 & 6

Time (minutes)	Average Temperature (C°)
0	25.55
15	27.05
30	28.575
75	33.475
90	35.45

C. Testing the code

To individually test our code, a proof of concept of the algorithm can be made by calculating the resistance of a different component through a similar circuit. As the thermistor–resistor configuration is simply a potential divider, we instead model its function through a 5kΩ potentiometer. We used a 16-bit **ADS1115** ADC[14] to construct Fig. 21 via breadboard, and monitored its output with the code as the potentiometer was adjusted. Due to the nature of the **ADS1115**, the reference voltage is internal and not explicitly defined, and it instead uses a

[14]Specific component is the Adafruit 1085. Mouser No: 485-1085

TABLE IX: Equivalent Data for Experiment III – Row temperatures

Row number	Temperature(°C)
1	28
2	28
3	29
4	29
5	30
6	32
7	35
8	37
9	40
10	41

TABLE X: Equivalent Data for Experiment III – Thermal Camera Row temperatures

Row number	Temperature(°C)
1	30.475
2	30.5
3	31.65
4	32.3
5	35.05
6	35.85
7	38.45
8	39.5
9	43.8
10	44.9

manually adjustable gain[15]. The code was modified to use equation (8), and results of the experiment can be found in Table XI.

[15]Default gain of the ADS1115 is 2/3x.

TABLE XI: Data from code testing

ADC Value Reading	V_O Reading (V)	Calculated Resistance (Ω)
17536	3.29	3.04
15984	3.00	100.00
15408	2.89	141.87
14384	2.70	222.22
13488	2.53	304.35
12384	2.32	422.41
10720	2.01	641.79
9264	1.74	896.55
8096	1.52	1171.05
7120	1.34	1462.69
6048	1.13	1920.35
5104	0.96	2437.50
4144	0.78	3230.77
2960	0.56	4892.86
2848	0.53	5226.42

X. Results, Discussion and Evaluation

A. Data Analysis

1) Equivalent to Experiment I: When comparing Table VII, Table VIII and the data for Experiment I, we can observe that there is a strong correlation between the data from the thermistors and the thermal camera. This can better be seen in Fig. 30.

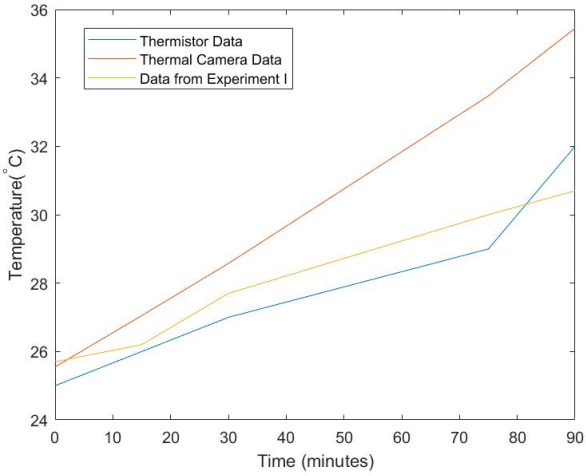

Fig. 30: Comparison between thermistors, thermal camera and Experiment I temperature results

Note that the temperature in the thermistor datasheet is given in intervals of five degrees, there-

fore estimation is required to monitor the exact values. It is important to notice that this is not critical for our project, as we are not concerned with the exact cell temperature, but rather monitoring a large increase.

From both devices we found the temperature of the cells to start around 25 degrees, which is the temperature of the environment before starting the experiment. Then, it can be appreciated in the above figure that the three sets of data increase at similar rates. However, the temperature found with the thermal camera tends to be higher than the thermistor counterpart. It can be clearly seen after 75 minutes where the difference between them is the highest, having a difference of almost 4.5 degrees.

One possible explanation for this is that the thermal camera has a limited battery which lasts for around one hour. As the battery gets depleted, the thermal camera can start to lose accuracy. Another reason this could happen is the aforementioned interval in the thermistor datasheet. Since temperature was given in intervals of five degrees, estimation is required to find the exact temperature.

Albeit there are some differences between the three sets of data, they do show a substantial similarity, with all of them showing a rather linear increase in the time interval. This proves that, at least in this situation, the designed PCB works well.

2) Equivalent to Experiment III: Comparing Table IX, Table X and the data for Experiment III in the cathode, it can be seen that, just like in the previous experiment, the three results are very similar. Fig. 31 is a bar graph showing the temperature per row from the three sets of data.

Firstly – as was observed in Experiment III – it can be seen that there is a big difference in temperatures between the first and last rows. Furthermore, comparing the data from all three tests shows that the results follow the same dynamic, with temperatures increasing per row and achieving a maximum value in the tenth one. Just like in the previous experiment, the thermistors tend to give a lower temperature than the thermal camera. This is probably due to all of the reasons mentioned earlier.

After these two tests, we can safely conclude that

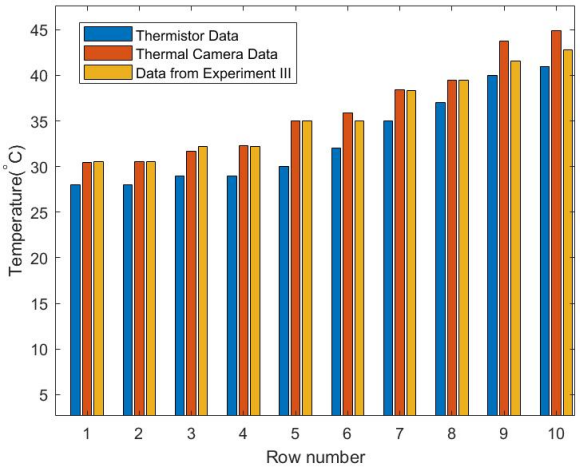

Fig. 31: Comparison between thermistors, thermal camera and Experiment III temperature results

our PCB works as intended[16]. The thermistors provide a voltage that reflect the true temperature inside the BRIC. While slightly inaccurate, we want to emphasize that knowing the exact cell temperature is unnecessary, therefore this is not a problem.

3) Testing the code: The results in Table XI signify the change in recorded voltage output as the potentiometer (and therefore the resistance) was adjusted. Calculating said resistance via the code reveals the negative relationship between the two variables – this is expected from the potential divider equation (7). As the potentiometer lacks the beta constant and response curve of a thermistor, we cannot calculate and analyse the temperatures from this test. However, previous results in the second testing experiment show an increase in voltage output with increasing temperature, which would have been due to the nature of the NTC thermistor and its decrease in resistance. While this is not a definitive conclusion, the supporting evidence from the previous experiment implies that similar trends and results would have been obtained had the communications with the ADCs worked.

[16]Of course, these tests were only performed in the 40–sensor configuration. Given that this design works, it it a safe assumption to believe the 27–sensor design would also work.

XI. Conclusion and recommendations

A. Future improvements

1) Updating components: As mentioned in the section above, the most immediate and significant change we can make to our PCB is implementing it with a different component choice. This would simply require discussing possible choices, selecting the optimal one and replacing the footprints on the PCB in Altium.

2) Machine Learning: During initial planning of our project we have discussed implementing a Machine Learning algorithm. Our idea was to give Alp the ability not only to measure current behaviour of cells, but also to predict, with relative accuracy, how the cells will behave in the future. This would be a useful addition to our project, as currently the capacity in which we can ensure cell protection is fairly limited. This is because the changes in cells can be sudden. Effectively this means that by the time the system flags a high temperature on one of the cells, it may already be damaged. With a working mathematical model, a machine learning algorithm could be able to analyse small changes in the thermistor's resistance and issue a warning about cells which are in potential danger.

B. Conclusion

All in all, we believe that we have succeeded at what we initially set out to do. We designed a PCB that allows for temperature monitoring within the BRIC. Although we were unable to create a final working product, we have managed to provide a framework for Alp Technologies such that they can properly implement it in the future if they desire to do so.

A successful implementation of our prototype in the BRIC will surely lead to both time saves as well as a decrease in cell waste. Given that the company works with recycled cells, this will result in a great net decrease in cell waste. Furthermore, Alp Technologies could add a Machine Learning algorithm to predict how cells will behave in the future.

From building 20 BRICs and one analyser board all the way to testing our final product, this project has given us a lot of knowledge and tools that we will most certainly use in the future. This experience has been a true pleasure for us and we can't wait to see how Alp Technologies develops in the years to come.

XII. Management

Following Alp Technology's recommendation, the group adopted the agile scrum methodology. This is a project management system that relies on completing smaller tasks, or sprints, in order to achieve the main goal. Each sprint lasts between two and four weeks, with daily talks between the group members to discuss progress and future steps.

Within the scrum team there is a scrum master, who is in charge of making sure everything runs smoothly and is up to date. Furthermore, the scrum master chairs the daily meetings to discuss progress and future steps [27].

In our group we all participated in the scrum team, with Juan Sigman being the scrum master. This management style allowed us to maintain a good organisation of the tasks to be completed and allowed us to finish everything on time.

The specific contributions by group member can be seen below:

Anas Baig: Anas mainly worked on the literature review. He would read relevant papers on the field and then update the group on any necessary knowledge we might need.

Emir Mukovic: Emir's main contribution to the project was during the PCB design section. He was our Altium expert, designing the schematic and PCB in the software.

Gerard Montblanch: Being a management student as well as an engineer, Gerard took care of the business side of the project, as well as being the second in command.

Nathaniel Williams: Nathaniel worked hard on the Arduino code involving the I^2C communication protocol.

Juan Sigman: Juan was the team leader and was involved in most tasks in the project. He made sure everything was on track and running smoothly, and helped out the rest of the group in anything they might need.

References

[1] Alp Technologies. M-BRIC — https://www.alp-technologies.com/mbric.

[2] IEA (2021), Renewable Power, IEA, Paris. https://www.iea.org/reports/renewable-power

[3] IEA (2021), Global Energy Review 2021, IEA, Paris https://www.iea.org/reports/global-energy-review-2021

[4] Muller, G. and La Camera, F. (2020). The Renewable Energy Transition in Africa. [online] Available at: https://www.irena.org/-/media/Files/IRENA/Agency/Publication/2021/March/Renewable_Energy_Transition_Africa_2021.pdf.

[5] African Development Bank Group (2018). Why Africa is the next renewables powerhouse. https://www.afdb.org/en/news-and-events/why-africa-is-the-next-renewables-powerhouse-18822#: :text=The%20International%20Renewable%20Energy%20Agency.

[6] Earth911 (2021). 20 Staggering E-Waste Facts. Earth911.com. Available at: https://earth911.com/eco-tech/20-e-waste-facts/.

[7] Dahunsi, F.M. (2013b). Conceptual framework for sustainable energy development in Africa. 2013 IEEE International Conference on Emerging Sustainable Technologies for Power & ICT in a Developing Society (NIGERCON).

[8] Charles, R.G., Davies, M.L., Douglas, P., Hallin, I.L. and Mabbett, I. (2019). Sustainable energy storage for solar home systems in rural Sub-Saharan Africa – A comparative examination of lifecycle aspects of battery technologies for circular economy, with emphasis on the South African context. Energy, 166, pp.1207–1215.

[9] Leng, F., Tan, C. & Pecht, M. Effect of Temperature on the Aging rate of Li Ion Battery Operating above Room Temperature. Sci Rep 5, 12967 (2015). https://doi.org/10.1038/srep12967

[10] X. Huang et al., "Lifetime Extension of Lithium-ion Batteries with Low-Frequency Pulsed Current Charging," in IEEE Journal of Emerging and Selected Topics in Power Electronics, doi: 10.1109/JESTPE.2021.3130424.

[11] Y. Liu, Y. G. Liao and M. -C. Lai, "Temperature Distribution on Lithium-ion Polymer Battery: From 12V Module to 48V Pack," 2020 IEEE Transportation Electrification Conference Expo (ITEC), 2020, pp. 240-245, doi: 10.1109/ITEC48692.2020.9161651.

[12] Huang, Y., Lu, Y., Huang, R., Chen, J., Chen, F., Liu, Z., Yu, X. and Roskilly, A.P. (2017b). Study on the thermal interaction and heat dissipation of cylindrical Lithium-Ion Battery cells. Energy Procedia, [online] 142, pp.4029–4036. Available at: https://www.sciencedirect.com/science/article/pii/S1876610217360630 [Accessed 16 Dec. 2021].

[13] Kantharaj, R. and Marconnet, A.M. (2019b). Heat Generation and Thermal Transport in Lithium-Ion Batteries: A Scale-Bridging Perspective. Nanoscale and Microscale Thermophysical Engineering, 23(2), pp.128–156.

[14] Qian, X., Xuan, D., Zhao, X. and Shi, Z. (2019). Heat dissipation optimization of lithium-ion battery pack based on neural networks. Applied Thermal Engineering, 162, p.114289.
InSitu Lee, C.-Y., Lee, S.-J., Tang, M.-S. and Chen, P.-C. (2011). In Situ Monitoring of Temperature inside Lithium-Ion Batteries by Flexible Micro Temperature Sensors. Sensors, 11(10), pp.9942–9950.

[15] Bhaskar, C.V.N., Pal, S. and Pattnaik, P.K. (2021). Recent advancements in fiber Bragg gratings based temperature and strain measurement. Results in Optics, 5, p.100130.

[16] Raijmakers, L.H.J., Danilov, D.L., van Lammeren, J.P.M., Lammers, M.J.G. and Notten, P.H.L. (2014). Sensorless battery temperature measurements based on electrochemical impedance spectroscopy. Journal of Power Sources, 247, pp.539–544.

[17] Chen, C. (2009). Evaluation of resistance–temperature calibration equations for NTC thermistors. Measurement, 42(7), pp.1103–1111.

[18] MATUS, Michael. Temperature measurement in dimensional metrology – Why the Steinhart-Hart equation works so well. Physikalisch-Technische Bundesanstalt (PTB), 2013. doi: 10.7795/810.20130620D

[19] Becker, J.A., Green, C.B. and Pearson, G.L. (1947). Properties and Uses of Thermistors-Thermally Sensitive Resistors*. Bell System Technical Journal, 26(1), pp.170–212.

[20] Keskin, A.Ü. (2005). A simple analog behavioural model for NTC thermistors including selfheating effect. Sensors and Actuators A: Physical, 118(2), pp.244–247.

[21] United Nations (2015). The 17 Sustainable Development Goals. [online] United Nations. Available at: https://sdgs.un.org/goals.

[22] Circuit-diagram.org. (2019). Circuit Diagram Web Editor. [online] Available at: https://www.circuit-diagram.org/editor/.

[23] www.flir.co.uk. (n.d.). FLIR ONE Pro Thermal Imaging Camera for Smartphones | Teledyne FLIR. [online] Available at: https://www.flir.co.uk/products/flir-one-pro/?vertical=condition-monitoringsegment=solutions.

[24] Gums, J. (2018). Types of Temperature Sensors. [online] www.digikey.co.uk. Available at: https://www.digikey.co.uk/en/blog/types-of-temperature-sensors.

[25] Anon, (n.d.). Types of Thermistors differences, NTC vs PTC thermistors. [online] Available at: https://enercorp.com/types-of-thermistors/.

[26] Electronics Hub. (2015). Thermistor Applications and Characteristics | PTC and NTC Thermistors. [online] Available at: https://www.electronicshub.org/thermistors-types-and-applications/#: :text=We%20can%20use%20PTC%20thermistors

[27] Sean, P. (2021). What Is Agile Scrum Methodology? - businessnewsdaily.com. [online] Business News Daily. Available at: https://www.businessnewsdaily.com/4987-what-is-agile-scrum-methodology.html#: :text=Agile.

[28] https://emckclac-my.sharepoint.com/:f:/g/personal/k1928978_kcl_ac_uk/Eo44ohQJjqxNmCbSvm48pUEBquPDnQiA-NhMtGPv9fSS1Q?e=eNYRtR

[29] ww.lithiumion-batteries.com. (n.d.). Cylindrical Vs Prismatic Cells. [online] Available at: https://www.lithiumion-batteries.com/cylindrical-vs-prismatic-cells.php.

[30] . Horiba, "Lithium-Ion Battery Systems," in Proceedings of the IEEE, vol. 102, no. 6, pp. 939-950, June 2014, doi:

[31] . Young, The Technical Writer's Handbook. Mill Valley, CA: University Science, 1989.

[32] u, Y., Vergori, E., Worwood, D., Tripathy, Y., Guo, Y., Somá, A., Greenwood, D. and Marco, J. (2021). Distributed thermal monitoring of lithium ion batteries with optical fibre sensors. Journal of Energy Storage, 39, p.102560.

[33] alsetti, C., Kapulla, R., Paranjape, S. and Paladino, D. (2021). Thermal radiation, its effect on thermocouple measurements in the PANDA facility and how to compensate it. Nuclear Engineering and Design, [online] 375, p.111077. Available at: https://www.sciencedirect.com/science/article/pii/S0029549321000297 [Accessed 13 Oct. 2021].

[34] . Liu, C. Zheng, C. Liu and P. W. T. Pong, "Experimental Investigation of a Johnson Noise Thermometry Using GMR Sensor for Electric Vehicle Applications," in IEEE Sensors Journal, vol. 18, no. 8, pp. 3098-3107, 15 April15, 2018, doi: 10.1109/JSEN.2018.2805309.

[35] ahiraei, F., Ghalkhani, M., Fartaj, A. and Nazri, G.-A. (2017). A pseudo 3D electrochemical-thermal modeling and analysis of a lithium-ion battery for electric vehicle thermal management applications. Applied Thermal Engineering, 125, pp.904–918.

[36] heng, Z., Ji, X. and Cahill, D.G. (2022). Battery absorbs heat during charging uncovered by ultra-sensitive thermometry. Journal of Power Sources, 518, p.230762.

[37] aijmakers, L.H.J., Danilov, D.L., Eichel, R.-A. . and Notten, P.H.L. (2019). A review on various temperature-indication methods for Li-ion batteries. Applied Energy, 240, pp.918–945.

Appendix A
Code

```
// Requires Wire library

#include <Wire.h>
#include <WiFi.h>

// Define the SDA and SCL pins for the I2C buses
const int I2C_SDA_0 = 23;
const int I2C_SCL_0 = 22;

const int I2C_SDA_1 = 21;
const int I2C_SCL_1 = 19;

// These ADCs use the I2C0 BUS  (I2Cone)
#define ADC_0 0x48
#define ADC_1 0x4A
#define ADC_2 0x49
// These ADCs use the I2C1 BUS  (I2Ctwo)
#define ADC_3 0x4B
#define ADC_4 0x48

// Create arrays to store the Addresses and Command bytes
//to write to the NCD9830
int ADC_ADDR[] = {ADC_0, ADC_1, ADC_2, ADC_3, ADC_4};
int ADC_COMM[] = {0x8C, 0xCC, 0x9C, 0xDC, 0xAC, 0xEC, 0xBC, 0xFC};

// Arrays to store ADC Readings and Temperature values
unsigned int ADC_ARRAY[10][4] = {0};
float TMP_ARRAY[10][4] = {0};

// Reference Voltage, Source Voltage, Max Value
//of ADC Reading (2^8 - 1), Resistor value in circuit
const float VREF = 2.5, VCC = 3.3, ADCMAX = 255, RST0 = 1000.0;
const float inv_TMP0 = 1/298.15, inv_BETA = 1/4500.0;

//WiFi Configuration
char ssid[] = "";          // Enter WiFi SSID here
char password[] = "";      // Enter Wifi Password here
char server[] = "pool.ntp.org";
const int gmtOffset = 0;  // Offset from GMT
const int dstOffset = 0;  // Enter 3600 if in Daylight Savings

TwoWire I2Cone = TwoWire(0); //I2C0 bus
TwoWire I2Ctwo = TwoWire(1); //I2C1 bus

void setup() {
```

```
    Serial.begin(9600);
    I2Cone.begin(I2C_SDA_0, I2C_SCL_0);
    I2Ctwo.begin(I2C_SDA_1, I2C_SCL_1);
}

void Read_ADC_Values() {
  // iterate over ADC Addresses 0 1 2
  for (int i = 0; i < 3; i++){
    //iterate over ADC Channels 0 1 2 3 4 5 6 7
    for (int j = 0; j < 8; j++){
      // Read from each ADC Channel and store value in the array
      I2Cone.beginTransmission(ADC_ADDR[i]);
      I2Cone.write(ADC_COMM[j]);
      I2Cone.endTransmission();
      I2Cone.requestFrom(ADC_ADDR[i], 1);
      if (I2Cone.available() == 1){
        if (j < 4){
          ADC_ARRAY[(8 - (2 * i))][3 - j] = I2Cone.read();
        }
        else{
          ADC_ARRAY[(9 - (2 * i))][7 - j] = I2Cone.read();
        }
      }
    }
  }
}
  // iterate over ADC Addresses 3 4
  for (int i = 3; i < 5; i++){
    for (int j = 0; j < 8; j++){
      I2Ctwo.beginTransmission(ADC_ADDR[i]);
      I2Ctwo.write(ADC_COMM[j]);
      I2Ctwo.endTransmission();
      I2Ctwo.requestFrom(ADC_ADDR[i], 1);
      if (I2Ctwo.available() == 1){
        if (j < 4){
          ADC_ARRAY[(8 - (2 * i))][3 - j] = I2Ctwo.read();
        }
        else{
          ADC_ARRAY[(9 - (2 * i))][7 - j] = I2Ctwo.read();
        }
      }
    }
  }
}

void Convert_ADC_Values() {
  for (int i = 0; i < 10; i++){
    for (int j = 0; j < 4; j++){
```

```
      // Rearrange ADCMAX/ADCVAL = VREF / VO and
      // voltage divider equation VO = VCC * R0/(Rt+R0) to find Rt
      float Rt = RST0 * ( (VCC * ADCMAX) / (VREF
      * (float)ADC_ARRAY[i][j]) - 1.0);

      // Use equation 1/T = 1/T0 +(1/B)*ln(R/R0) ,
      //convert Temperature value from kelvin to Celsius
      float logR_R0 = log(Rt / RST0);
      TMP_ARRAY[i][j] = 1.0 / ( inv_TMP0 + (inv_BETA * logR_R0) );
      TMP_ARRAY[i][j] -= 273.15;
    }
  }
}

void Display_TMP_Values() {
  // First displays "Battery Temperature Recording ( C ) - yy-mm-dd
hh:mm:ss"
  Serial.print("Battery␣Temperature␣Recording␣( C )␣␣-␣␣");

  Serial.print(&timeinfo, "%F");
  Serial.print("␣␣");
  Serial.print(&timeinfo, "%T");
  Serial.print("␣UTC");
  Serial.print("\n\n");

  // Then displays the temperature values
  for (int i = 0; i < 10; i++){
    for (int j = 0; j < 4; j++){
      Serial.print(TMP_ARRAY[i][j]);

      Serial.print("\t");
    }
    Serial.print("\n");
  }
  Serial.print("\n");
}

void loop() {
  // put your main code here, to run repeatedly:
  Read_ADC_Values();
  Convert_ADC_Values();
  Display_TMP_Values();
}
```

Appendix B
Testing the design data – Experiment I

A. ADC voltages vs Time – Rows 5 and 6

TABLE XII: ADC voltages vs Time - rows 5 & 6

Time(minutes)	Average Voltage (V)
0	1.655
15	1.765
30	1.81
75	1.84
90	1.88

Appendix C
Testing the design data – Experiment II

A. Full data

TABLE XIII: Full BRIC thermistor voltages

	Column 1 Voltage (V)	Column 2 Voltage (V)	Column 3 Voltage (V)	Column 4 Voltage (V)
Row 1	1.81	1.81	1.81	1.82
Row 2	1.82	1.81	1.81	1.81
Row 3	1.84	1.84	1.83	1.83
Row 4	1.85	1.85	1.84	1.83
Row 5	1.86	1.86	1.85	1.85
Row 6	1.91	1.91	1.91	1.92
Row 7	2.05	2.04	2.04	2.04
Row 8	2.07	2.07	2.09	2.09
Row 9	2.23	2.23	2.21	2.23
Row 10	2.26	2.26	2.28	2.28

B. Data from thermal camera

TABLE XIV: Temperature vs Time - outside cells

Time = 90	Column 1 Voltage (V)	Column 2 Voltage (V)	Column 3 Voltage (V)	Column 4 Voltage (V)
Row 1	30.3	-	-	30.5
Row 2	20.5	-	-	30.5
Row 3	31.7	-	-	31.6
Row 4	32.4	-	-	32.2
Row 5	35.1	-	-	35.0
Row 6	35.8	-	-	35.9
Row 7	38.4	-	-	38.5
Row 8	39.6	-	-	39.4
Row 9	43.8	-	-	43.8
Row 10	44.9	-	-	44.8

Appendix D
Circuit schematics

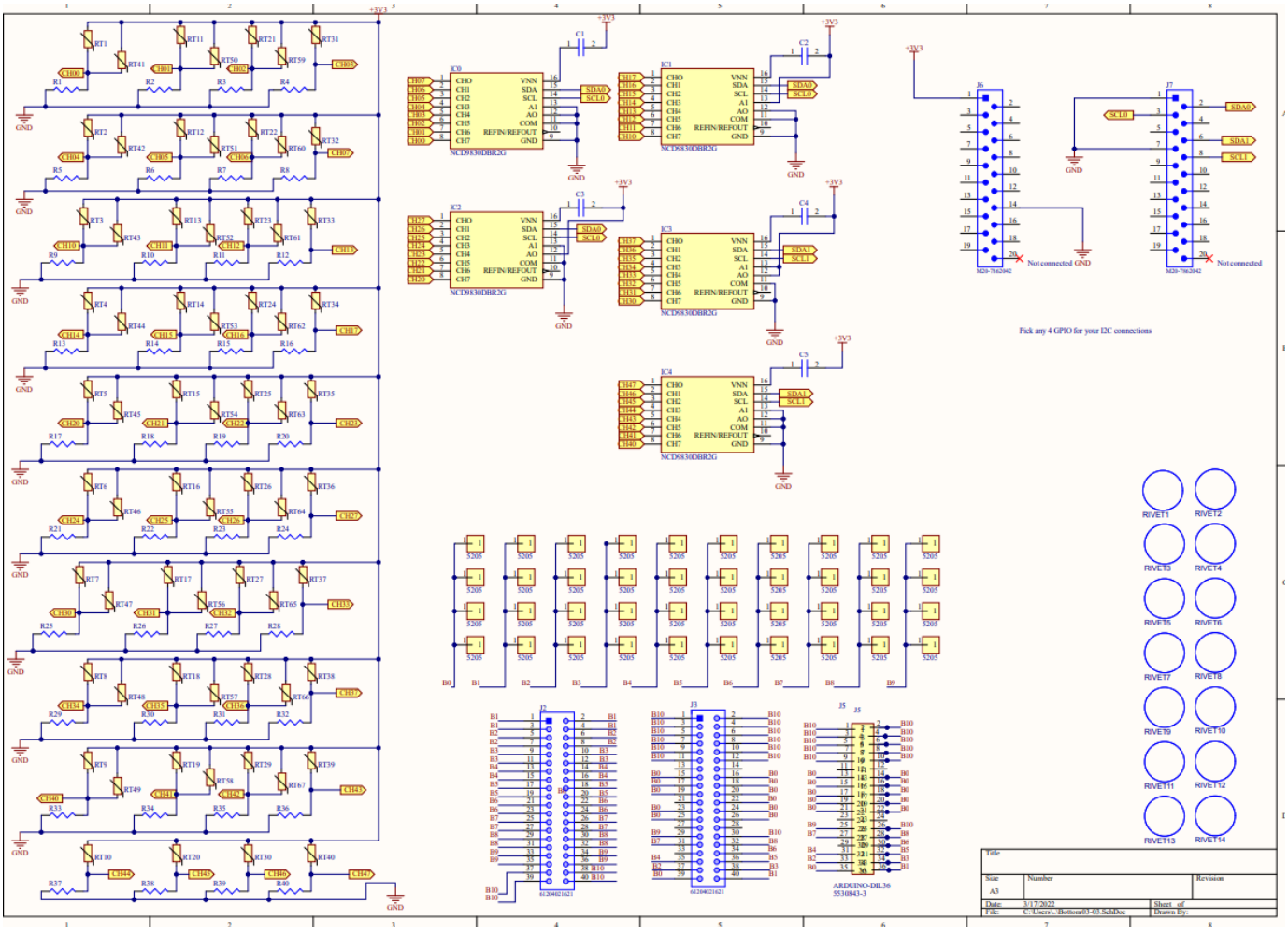

Fig. 32: Full Schematic